Computational Investigation of Drag Reduction on An Ahmed Body Using Square Grooves

By

Rawail Haseem

Reg No. 00000172079

Session 2016-18

Supervised by

Dr. Adeel Javed

A Thesis Submitted to the US-Pakistan Center for Advanced Studies in Energy in partial fulfillment of the requirements for the degree of MASTER of Science in

THERMAL ENERGY ENGINEERING

US-Pakistan Center for Advanced Studies in Energy (USPCAS-E)

National University of Sciences and Technology (NUST)

H-12, Islamabad 44000, Pakistan

September 2020

THESIS ACCEPTANCE CERTIFICATE

Certified that final copy of MS/MPhil thesis written by **Mr. Rawail Haseem**, (Registration No. 172079), of USPCS-E (Institute) has been vetted by undersigned, found complete in all respects as per NUST Statues/Regulations, is within the similarity indices limit and is accepted as partial fulfillment for the award of MS/MPhil degree. It is further certified that necessary amendments as pointed out by GEC members of the scholar have also been incorporated in the said thesis.

Signature: _____

Name of Supervisor Dr. Adeel Javed

Date: _____

Signature (HoD TEE): _____

Date: _____

Signature (Dean/Principal): _____

Date: _____

Certificate

This is to certify that work in this thesis has been carried out by **Mr. Rawail Haseem** and completed under my supervision in US-Pakistan Center for Advanced Studies in Energy (USPCAS-E), National University of Sciences and Technology, H-12, Islamabad, Pakistan.

Supervisor: _____

Dr. Adeel Javed
USPCAS-E
NUST, Islamabad

GEC member # 1: _____

Dr. Majid Ali
USPCAS-E
NUST, Islamabad

GEC member # 2: _____

Dr. Adeel Waqas
USPCAS-E
NUST, Islamabad

GEC member # 3: _____

Dr. Adnan
RCMS
NUST, Islamabad

H.O.D.- (TEE) : _____

Dr. Adeel Javed
USPCAS-E
NUST, Islamabad

Principal/ Dean _____

Dr. Adeel Waqas
USPCAS-E
NUST, Islamabad

Dedication

I would like to dedicate this research to my family who supported me to conduct this research study, my teacher who helped and guided me throughout my research.

Acknowledgement

I am thankful to Almighty Allah who gave me the strength to complete my research. I am forever in debt to my advisor Dr. Adeel Javed for his guidance, encouragement and for believing in me at every step of this journey.

I am grateful to my committee members Dr. Majid Ali, Dr. Adeel Waqas and Dr. Adnan for their support. And finally, I would like to thank my friends for their continuous support that helped me in completing this study.

Abstract

In Pakistan 96% of the freight transportation is done through trucks. These bluff body vehicles do not have a streamlined shape and hence have a high pressure drag. This aerodynamic pressure drag causes up to 15-20% extra fuel consumption. Aerodynamic drag can be reduced by using different passive techniques of fluid flow control. In this paper, the influence of square grooves on the passive drag reduction has been evaluated. In the first phase simulations have been performed to investigate the skin friction coefficient of smooth flat plate with square groove in it. These grooves are placed transverse to the incoming flow. This results in increasing the friction drag along the boundary causing the transition of laminar flow to turbulent. Similar technique is used in the second phase around a square back Ahmed Body and then finally on a scaled model of Pakistani dumper truck. The study has been conducted with computational fluid dynamics (CFD) simulations using ANSYS Fluent. Unsteady Reynolds Averaged Navier-Stokes (URANS) formulation has been employed in the simulation. The focus of this study is to help the transportation sector of Pakistan by making efficient aerodynamic design. This study is applicable to Pakistani heavy transport vehicles with an intention to reduce the high fuel consumption which is caused due to high pressure drag

Keywords: Ahmed Body; CFD; Flat Plate; Square Groove

Table of Contents

List of Figures

List of Tables

List of Journal/Conference Papers

1. **Rawail Haseem**, A. Javed “Computational Investigation of Drag Reduction on an Ahmed Body Using Square Grooves” International Conference on Renewable, Applied and New Energy Technologies, November 2018, Air University Islamabad

Chapter 1: Introduction

1.1 Background and Scope

Road freight transport is one of the most important components of the transport sector within a developing country. 96 percent of freight movement is done through road transport, making it the backbone of Pakistan's transport system. Existing studies on Pakistan's road transport sector remains, for the most part, incomplete and obsolete. Credible information on this sector is still hard to find. There is a difference in the total number of trucks with multiple research quoting different statistics [1]. Pakistan's truck fleet consists of 65-70% to single or double axel trucks. According to National Highway Authority, there were only 1,36000 commercial trucks registered (3% of total vehicles), that were on Pakistani roads in 1995 [2].

Our focus in this research is the fastest growing segment is the road transport sector i.e. the freight segment. The relevance of the road freight sector in national economy is unquestionable. In Pakistan, Transport, Logistics and Communication (TLC) sector contributed 13.3% to GDP in 2018-19, out of which 62% was contributed by road transport sector and provides employment to 3.1 million people [3]. Freight transportation through railway has decreased to 4% only [5]. The productivity of Pakistan Railway is only one-eighth and one-third of China and India, respectively [6].

From *Figure 1* [7] we can see that the percentage increase in the number of registered trucks, annually, has been small over the past 15 years. The most notable increase was 9% in 2002 and 7% in 2012.

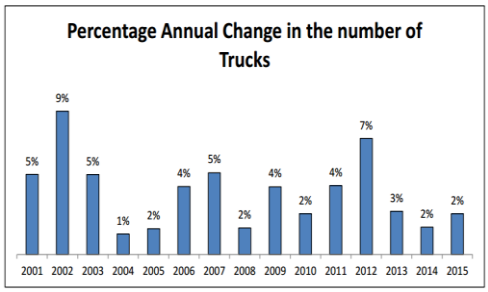

Figure 1 Percentage Annual Change in the Number of Trucks

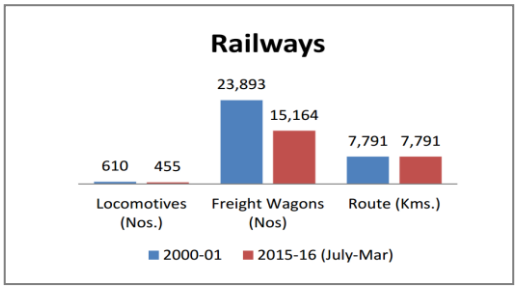

Figure 2 Decrease in Freight through Railway (37%)

Road freight is anticipated to grow consistently particularly in CPEC scenario and because of Pakistan's geo-strategic location, which allows it to facilitate its road freight at its ports to other countries. There is a severe need to streamline the trucking sector.

Single ownership of old Bedford *(Figure 3)* and Dumper trucks *(Figure 4)* is common phenomenon which cannot be overcome in the present environment as with increasing fuel prices and competition, the sector becomes more and more marginalized. Informal financing with 100% interest rate, constraints the driver-owner from switching to modern vehicles [8].

Figure 3 Old Bedford Trucks

Figure 4 Pakistani Dumper Truck

These trucks are imported in completely knocked down (CKD) forms and assembled locally as there is no truck production company. Most trucks are strengthened after they are imported, to take heavier loads. Original Bedford trucks had the capacity to carry a weight of 07 tons [9] but are strengthened by modifying the chassis, axle spring and engine compartment.

These bluff body (trucks) cause the air to separate, causing a major pressure to drop. This generates a large wake. The inability of the flow to reach the back of the vehicle, past its sharp edges and the lack energy becomes the cause of the separation. The resistance to air flow increases fuel consumption by 15- 20 percent [10]. It is estimated that 35% of fuel is consumed by Pakistan's transport sector [11].

There are two types of drag, one is profile drag which is caused by its surface area and the second one is skin friction drag [12].

1.2 Summary

These locally manufactured Pakistani trucks are embellished with art, but their design is a nightmare in vehicle aerodynamics due to its blunt shape and sharp edges. The main goal of this research is to establish the aerodynamic impact of square grooves on a Bedford or a Dumper truck and to optimize the groove design such that it could be used on locally manufactured trucks that would result is fuel saving.

1.3 References

[1] N. K. Co, N. K. Co, A. Corporation, and A. Corporation, "PAKISTAN TRANSPORT PLAN STUDY IN THE ISLAMIC REPUBLIC OF PAKISTAN Final Report," *Transport*, no. March, 2006.

[2] The international Trade Centre, "Road Freight Transport Sector &Emerging Competitive Dynamics," p. 39, 2012.

[3] AASA Consulting, "Bankability of the Transport Sector in Pakistan." Karandaaz, Pakistan, 2018-19.

[4] Government of Pakistan, "Pakistan Economic Survey," *Pakistan Econ. Surv. 2017-18*, p. 432, 2018.

[5] F. B. of S. GoP, "Pakistan Statistical Yearbook," 2008.

[6] P. C. G. O. PAKISTAN, "Framework for Economic Growth," no. May, 2011.

[7] Amnah Imtiaz E, "SHORT ROUNDUP ON TRANSPORT INFRASTRUCTURE IN Pakistan," 2016.

[8] MoIP&SI/EDB, "Industry Status For Trucking Sector," pp. 13–14.

[9] J. L. Hine and A. S. Chilver, "Pakistan road freight industry: an overview," *Res. Rep. - UK Transp. Road Res. Lab.*, no. RR 314, 1991.

[10] C. Pevitt, H. Chowdury, H. Moriaand, and F. Alam, "A computational simulation of aerodynamic drag reductions for heavy commercial vehicles," *Proc. 18th Australas. Fluid Mech. Conf. AFMC 2012*, no. December, pp. 3–6, 2012.

[11] S. P. Systems, "Major Issues: □," pp. 31–41, 2013.

[12] A. Altaf, A. A. Omar, and W. Asrar, "Passive drag reduction of square back road vehicles," *Journal of Wind Engineering and Industrial Aerodynamics*, vol. 134. pp. 30–43, 2014.

Chapter 2: Literature Review

The importance of energy conservation has been a driving force behind the ongoing research that will reduce the drag on transport vehicles. Passive control of the flow field around the body may result in aerodynamic drag reduction and a conforming performance enhancement.

Surface roughness has been widely investigated as a means of modifying the turbulent boundary layer. In transverse square grooves it is anticipated that circulating vortex is generated because of low-pressure area established instantly downstream. It helps in prolonging the turbulent development in the boundary layer [1]. In the case of a 2-dimensional flow, as the shear wall stress approaches to zero the point reaches where the flow separation takes place. The flow changes into turbulent [2]. Passive and active maneuvering of the flow field may produce drag reduction which causes increase in the performance.

Not in distant past, friction drag reduction methods have gained popularity in relation to less fuel consumption in aircrafts and submarines. Reduction using riblets have drawn more attention due to their greater potential of reducing drag.

2.1 Flat Plate

Many studies have concentrated their focus on riblets because of its potential drag reduction. Square grooves are comparatively simpler to develop. These 2-dimensional square grooves are placed in transverse to the incoming flow. They are more suitable for any further optimization, and when added together. Refrigeration systems, plate heat exchangers and other engineering equipment's use large grove designs [3]. Whereas bearings, automobiles, braking system, and high-pressure equipment's use microscopic grooves. Contradictory results have been recorded regarding the effectiveness of square grooves [2].

The effects of square grooves in fluid dynamics are far from being understood. Pritanshu [4] found that the distance between the grooves had a strong influence over the drag coefficient while C. Tay [5] investigated that with the increase in the coverage area, the drag reduction also increased.

Veldhuis [6] says that the drag reduces as the wall shear stress lessens for shallow dents. *Figure 5* explains us flow remains attached for shallow while the deeper dent displays separation.

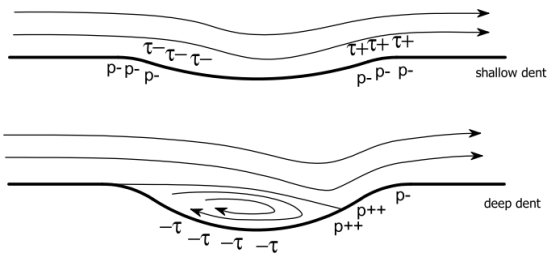

Figure 5 Friction and Pressure Drag effects in a surface Dent [6]

Choi and Fujisawa (1993) concluded that the effect of the grooves at the higher Reynold number is much more significant, with the largest groove (20 mm) having the most effect on the boundary layer while ignoring the pressure drag effect on the walls [7].

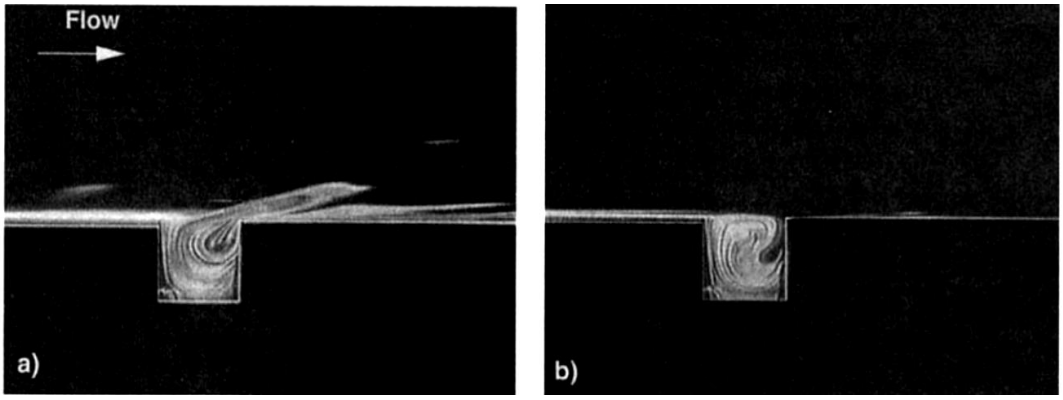

Figure 6 a) Typical outflow b) Typical Inflow [6]

Pearson (1997) gathered that momentum exchange is required in order to reduce the skin friction drag [8]. He captured an overshoot in skin friction coefficient just downstream of the groove followed by an undershoot and an oscillatory relaxation back to the smooth-wall value.

Tani et al. (1987) found that the skin-friction on a smooth surface with and without the square grooves was different over a certain range of Reynolds number [9]. Sutardi and Ching (1999) reported that there is a strong link between the wake parameter (π) and C_f distributions at R_θ (Reynolds number based on θ) 3000 [10].

2.2 Ahmed Body

The Ahmed Body is used as a reference model for fundamental studies of bluff body aerodynamics. In this study a base line drag value is obtained for a Dumper Truck using a Square Back Ahmed Body in Ansys Fluent and the drag reduction through different modifications in the groove design along the Dumper Body are compared.

The market does not appreciate frequent launching of new models. New truck model demands more time to design and are not affordable for Pakistani buyers. According to a study conducted in Pakistan, aerodynamic pressure drag leads up to 15-20 % of extra fuel consumption [11]. There is a probability that the aerodynamic drag of Dumper Trucks in developing countries like Pakistan can lead to great profit by reducing the fuel consumption.

The two main components of Aerodynamic drag are pressure drag which contributes up to 80% of the total drag and skin friction drag. Hucho in his study states that almost 50% of the total fuel consumption of a vehicle is caused by the aerodynamic drag [12]. W. Mayers el al say that by optimizing the shape of the vehicle we can improve the fuel efficiency [13].

We are going to focus on passive control in this study. The corner of vehicles with square back causes the air fleeting by its body to separate, leading to a massive fall in the pressure that produces a long wake behind the vehicle [14], [15]. The target of this study is to develop control solution to reduce the aerodynamic drag of the vehicle without forcing a change in the original design of the body. The success depends upon controlling the point where the separation along the body occurs. Recirculation area at the rear end of the body can be cut down by installing separation accessories at the back or the front of the body.

Experimental investigation using a deflector were carried out by Fourrie [16]. The study confirms that we can control the development of wake, depending on the angle of its deflector. Up to 9% of drag reduction was achieved by Fourrie. Investigation on full sized truck were carried out by Muhamed Kassin and Fhilippone [17]. They found out that every part of the truck contributes to the total drag and concluded that retrofitting is only suitable when vehicle is travelling at high speed. J. Ha [18]

observed a significant decrease in drag of a pickup truck by retrofitting a downward flap at its rear end.

Intriguing results were achieved with grooves positioned along the boundary, transverse to the incoming flow [19], [20]. This creates a force along the boundary layer which helps shift the separation point resulting in a decrease in pressure drag and decreasing the aerodynamic drag is another effective solution [14], [21]. Besides, the use of artificial rough surface achieves up to 50% reduction in drag. Turbulent laminar transition can also be rushed by using self-adapting surfaces made of special coating [22], [23]. The flow is naturally turbulent in automobile aerodynamics; thus the impact is very low.

2.3 Summary

50% of the fuel consumption caused by the drag of a vehicle. Failure to recover the pressure in the wake region for square back bodies contributes greatly, in increasing the aerodynamic drag.

This study emphasizes on the concept of flow separation. Numerous methods of controlling the flow separation have been explored. Reducing the aerodynamic drag with conventional passive control techniques proposes a reasonably less expensive solution to progress fuel effectiveness.

2.4 Reference

[1] P. B and R. Elavarasan, “The effect of a square groove on a boundary layer,” 1995.

[2] R. Wahidi, W. Chakroun, and S. Al-Fahed, “The behavior of the skin-friction coefficient of a turbulent boundary layer flow over a flat plate with differently configured transverse square grooves,” *Exp. Therm. Fluid Sci.*, vol. 30, no. 2, pp. 141–152, 2005.

[3] D. M. Bushnell and J. N. Hefner, *Viscous Drag Reduction in Boundary Layers*. .

[4] P. Ranjan, A. R. Paul, and A. P. Singh, “Computational analysis of frictional drag over transverse grooved flat plates,” vol. 3, no. 2, pp. 110–116, 2011.

[5] C. Tay, “Determining the Effect of Dimples on Drag in a Turbulent Channel Flow,” no. January, pp. 1–12, 2011.

[6] L. L. M. Veldhuis and E. Vervoorty, “Drag effect of a dented surface in a turbulent flow,” *Collect. Tech. Pap. - AIAA Appl. Aerodyn. Conf.*, no. June, pp. 1–12, 2009.

[7] Sutardi and C. Y. Ching, “Effect of different sized transverse square grooves on a turbulent boundary layer,” *Exp. Fluids*, vol. 34, no. 2, pp. 261–274, 2003.

[8] B. R. Pearson, R. Elavarasan, and R. A. Antonia, “The response of a turbulent boundary layer to a square groove,” *J. Fluids Eng. Trans. ASME*, vol. 119, no. 2, pp. 466–469, 1997.

[9] I. Tani, H. Munakata, A. Matsumoto, and K. Abe, “Turbulence Management by Groove Roughness,” *Turbul. Manag. Relaminarisation*, pp. 161–172, 1988.

[10] Sutardi and C. Y. Ching, “Effect of a transverse square groove on a turbulent boundary layer,” *Exp. Therm. Fluid Sci.*, vol. 20, no. 1, pp. 1–10, 1999.

[11] Amnah Imtiaz E, “Short RoundUp on Transport Infrastructure in Pakistan,” 2016.

[12] T. Morel, “Aerodynamics of Road Vehicles.,” *Fuel Econ Road Veh Powered by Spark Ignition Engines*, pp. 335–392, 1984.

[13] W. Mayer and G. Wickern, “The New Audi A6/A7 Family - Aerodynamic Development of Different Body Types on One Platform,” *SAE Int. J. Passeng. Cars - Mech. Syst.*, vol. 4, no. 1, pp. 197–206, 2011.

[14] R. S. Khan and S. Umale, “CFD Aerodynamic Analysis of Ahmed Body,” *Int. J. Eng. Trends Technol.*, vol. 18, no. 7, pp. 301–308, 2014.

[15] G. Vehicle, C. Bruneau, and E. Creus, “Analysis of the Active and Passive Drag Reduction Strategies Behind a Square Back Analysis of the Active and Passive Drag Reduction Strategies Behind a Square Back Ground Vehicle,” no. August 2016, 2018.

[16] G. Fourrié, L. Keirsbulck, L. Labraga, and P. Gilliéron, “Bluff-body drag

reduction using a deflector," *Exp. Fluids*, vol. 50, no. 2, pp. 385–395, 2011.

[17] Z. Mohamed-Kassim and A. Filippone, "Fuel savings on a heavy vehicle via aerodynamic drag reduction," *Transp. Res. Part D Transp. Environ.*, vol. 15, no. 5, pp. 275–284, 2010.

[18] H. J, J. S, and S. Obayashi, "Drag Reduction of a Pickup Truck By a Rear Downward Flap," *Int. J. Automot. Technol.*, vol. 13, no. 2, 2010.

[19] C. Bruneau, E. Creusé, D. Depeyras, P. Gilliéron, and I. Mortazavi, "Computers & Fluids Coupling active and passive techniques to control the flow past the square back Ahmed body," *Comput. Fluids*, vol. 39, no. 10, pp. 1875–1892, 2010.

[20] "Effect of compressibility on the global stability of axisymmetric wake flows," vol. 660, pp. 499–526, 2010.

[21] C.-H. Bruneau, I. Mortazavi, and P. Gilliéron, "Passive Control Around the Two-Dimensional Square Back Ahmed Body Using Porous Devices," *J. Fluids Eng.*, vol. 130, no. 6, p. 061101, 2008.

[22] P. W. Bearman and J. K. Harveyt, "Control of Circular Cylinder Flow by the Use of Dimples," vol. 31, no. 10, pp. 2–5, 1993.

[23] B. Pw, "Investigation of the flow behind a two-dimensional model with a blunt trailing edge and fitted with splitter plates," vol. 21, pp. 241–255, 1965.

Chapter 3: Methodology

The literature review suggests us a large range of methods and techniques to decrease the drag coefficient of a vehicle. Here in Pakistan, no work has been done to investigate the influence of different shapes at the square body of a dumper truck.

Aerodynamics of a vehicle can be tested through Road testing, utilizing Computational Fluid Dynamic (CFD) tools and by means of wind tunnel test. In this study we are sticking with CFD tools. Numerical methods are used in CFD to analyze the fluid flow. The very first and most common question that comes to the mind is that why do we need to use CFD when we have wind tunnels? For wind tunnel experiments we first must design the model, fabricate it and then perform the wind tunnel test. For even a slight change in the design it would have to be fabricated again whereas in the case of CFD analysis modifying the shape of your model for desired results is very convenient and less expensive.

In the first phase two different configurations of flat plate are simulated and validated through literature. These two configurations consist of: 1) Flat plat with smooth wall, 2) Flat Plate with single square groove. In the second phase these configurations of grooves are simulated on an Ahmed Body [1] and a Pakistani dumper truck. The objective of this paper is to control or reduce the separation area in the wake. A 2 and 3-dimensional study on Ahmed body is performed using Design of Experiment in which we concentrate on the total pressure gradient that governs the aerodynamic drag of Square Back Ahmed Body, which is a simplified form of a Dumper Truck.

Here the flow control is achieved by means of eight different configurations of Transverse Square grooves, which are inserted on the surface of the body. These square grooves modify the boundary layer effect as it changes the stress forces [2]. The goal is to show how well positioned transverse grooves and their geometry can modify the wake.

Design of experiments (DOE) was used for decreasing the number of experiments. DOE is a very proactive technique. What it envisions is that you actually adjust your process based on certain factors and you make very precise and well-coordinated

adjustments and in doing so we are able to see what happens to the output as we juggle the inputs but we do it in a controlled fashion.

In the following we give various results of different configuration of the flat plate and the flow on square back Ahmed Body. We carefully analyze these results and assess the effect of Square Grooves in the flow around the body.

3.1 Simulation Setup and Geometrical Dimensions

3.1.1 Flat Plate

3.1.1.1 *Flat Plate with Smooth Wall and a Single Square groove*

A flat plate and its domain are modeled in ANSYS Design modular in XY-plane. A simple rectangular domain was generated with a length of 1.75m and the height of 1m with an inlet velocity of 22.22 meter per second. This rectangular domain will act as a far field, the inlet and the outlet. Quadrilateral face meshing is applied on the surface along with edge sizing, for all edges and the type of mesh is changed to number of divisions. To achieve a finer mesh close to the plate as we have to simulate the boundary layer, we introduce the biasness factor. We expect a lot of singularities close to the plate rather than in the far field.

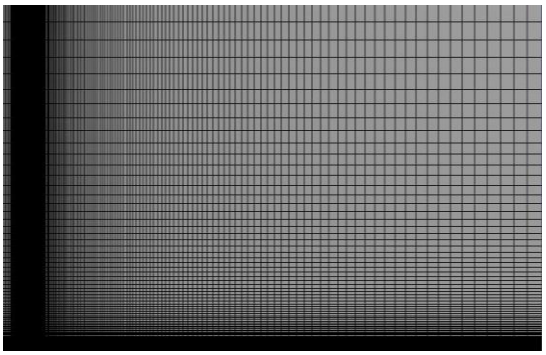

Figure 7 Flat Plate Smooth Wall Mesh

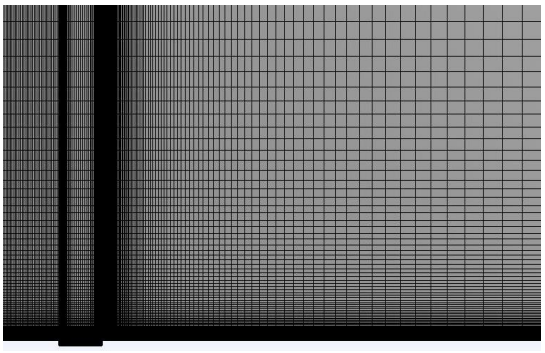

Figure 8 Flat Plate with Square Groove (Mesh)

Figure 7 and *Figure 8* displays the domain and the mesh generated for the simulation of flat plate with smooth wall and single square groove respectively. *Table 1* and *Table 2* present us the geometrical dimensions of the domain in which the simulation takes place and the boundary conditions.

Table 1 Boundary Conditions and Geometrical Dimension

Mesh Properties	***Parameter***
Domain Length	1.75m
Domain Height	1m
Plat Length	1.7m
Turbulent Intensity	5%
Turbulent Viscosity Ratio	10
Elements	46,500
Physics Properties	***Parameter***
Turbulence Model	K-Omega SST
Flow Characteristics	Transient
Inlet Velocity	22.22 m/s
Method	SIMPLE Pressure-Velocity Coupling

Table 2 Boundary Conditions and Geometrical Dimension

Mesh Properties	***Parameter***
Domain Length	1.75m
Domain Height	1m
Plat Length	1.7m
Groove Depth	0.014m
Groove Length	0.14m
Turbulent Intensity	5%
Turbulent Viscosity Ratio	10
Physics Properties	***Parameter***
Turbulence Model	K-Omega SST
Flow Characteristics	Transient
Inlet Velocity	22.22 m/s
Method	SIMPLE Pressure-Velocity Coupling

3.1.1.2 *Grid Independence*

Once the domain was modelled, mesh independence test was performed with a varying coarseness to determine the best mesh for the study. It is generally assumed that a sophisticated mesh with a higher number of elements lead to more accurate results but at the same time it requires longer processing time. *Table 3* displays the grid test results.

Table 3 Grid Independence Test for Flat Plate

Number of Elements	***Pressure Coefficient (C_f)***
20,098	0.357
59,998	0.545
90,298	0.547

3.1.2 Ahmed Body

The Ahmed body is used to study the vital flow characteristics around an automobile [3]. Once the numerical model in validated, it is used to design new models of the car. It is made up of a round shaped front part attached with a rectangular body which connects to the slanted plane at the rear end. The shape and dimensions of an Ahmed Body are shown in *Figure 9*.

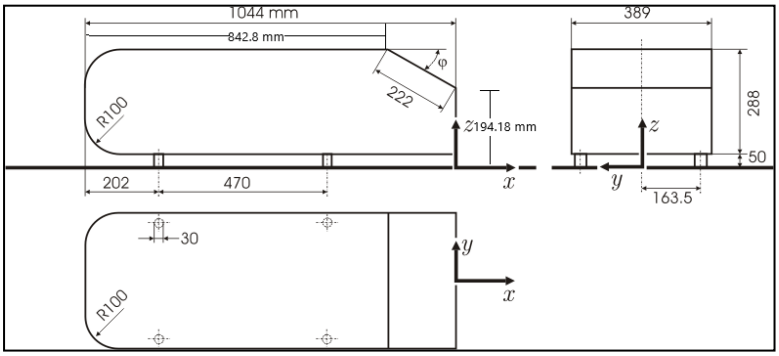

Figure 9 Schematic of Ahmed Body in Millimeters

3.1.2.1 *Two-Dimensional Ahmed Body*

From the layout provided in *Figure 9*, top view of two 2-dimensional Ahmed body with a square back are designed in Solidworks and are simulated in ANSYS Fluent 16. One with a smooth wall and the other with square grooves at the rear end. *Figure 10* shows the geometry of an Ahmed body with smooth walls.

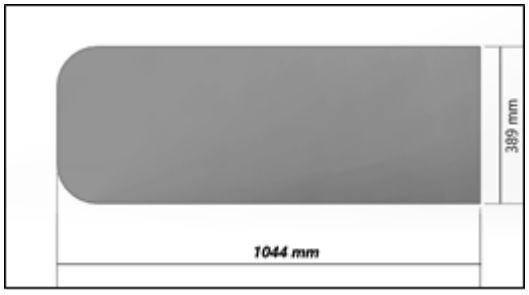

Figure 10 Ahmed Body with Smooth wall

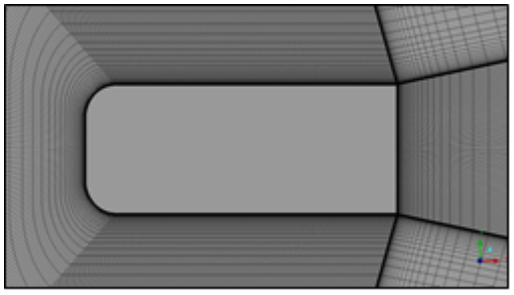

Figure 11 Ahmed Body with Smooth wall Mesh

This model was exported with IGS extension in ANSYS Workbench and structured meshing was done in ICEM *(Figure 11)*. The computational domain starts 2L in front of the model and extends to 7L behind the model. The height and length of the domain are 7.002 meters and 10.44 meters, respectively. First layer thickness near the body surface is kept 0.000016m.

Figure 12 shows the geometrical configuration of an Ahmed body with square grooves which was developed as a scaled down reference model of the dumper trucks hauling the roads of Pakistan. It was later kept as a baseline model for DOE with groove length of 70 mm, depth of 15 mm and 25 mm space between two grooves.

Same configuration of computational domain is used for the grooved body as was used for smooth body. First layer thickness 0.000016m.

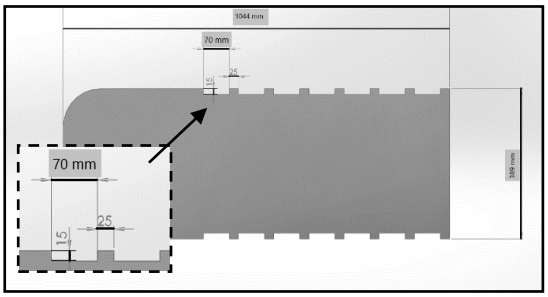

Figure 12 Ahmed Body with Square Grooves (Baseline)

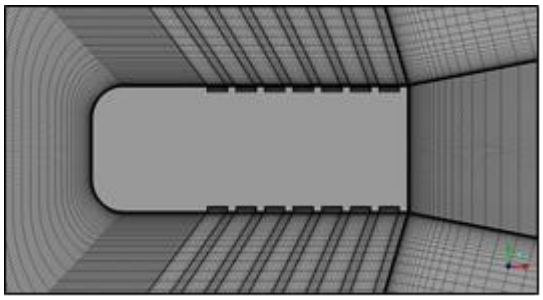

Figure 13 Ahmed Body Mesh with Square Grooves

The mesh was made finer along the body like the one made for flat plate geometry, to study the phenomena near the body rather in the far field. Smooth transition between the last boundary layer and core element is assured as seen in the *Figure 13*.

Grid independence test was undertaken for the Ahmed body with smooth wall and a maximum variation of 10% was found between the coarsest and the finest mesh. The results are shown in *Table 4* and *Graph 1*.

Table 4 Grid Independence of Ahmed Body with Smooth walls

Number of Elements	***Coefficient of Drag (C_d)***
90,002	0.371
119,898	0.408
134,998	0.412
149,563	0.408

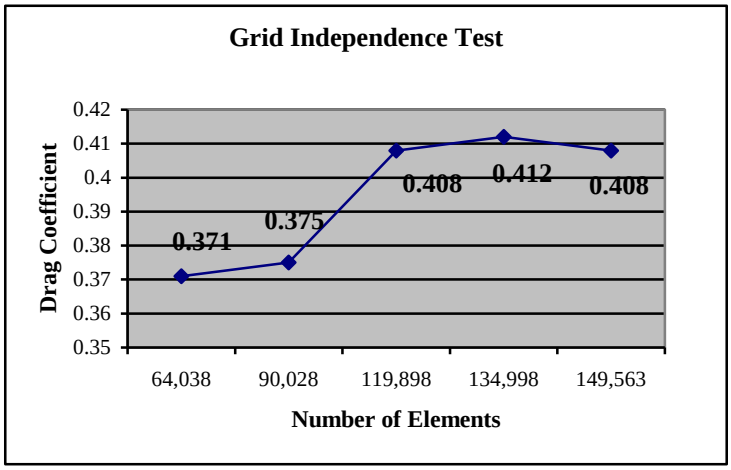

Graph 1 Grid Independence Smooth wall Ahmed body

3.2 Design of Experiment (D.O.E)

DOE method was used for decreasing the number of experiments. DOE is a very proactive technique. What it envisions is that you actually adjust your process based on certain factors and you make very precise and well-coordinated adjustments and in doing so we are able to see what happens to the output as we juggle the inputs but we do it in a controlled fashion.

The optimization of design in automotive is always one of the top concerns. In this paper the dimensions of the square grooves at the back of a dumper truck are defined as the performance evaluation index, whereas the depth, the length and the height of the groove are defined as the input variables.

DOE is a very proactive technique. What it envisions is that you actually adjust your process based on certain factors and you make very precise and well-coordinated adjustments and in doing so we are able to see what happens to the output as we juggle the inputs but we do it in a controlled fashion.

3.2.1 The Definition of Outputs and Inputs (Responses and Factors)

Generally, the evaluation indexes of a dumper truck include engine power, fuel economy, strength, compactness, durability but in this case the drag or the coefficient of drag will be out response (Dependent Variable).

Considering the feasibility of modeling in our design, we chose total length of the groove, the space in between the two grooves and the depth as the main input variables (Independent Variable).

3.2.2 Full Factorial DOE

Firstly, the input variable values are set (see *Table 5*). Two levels were assigned to each factor. A complete factorial design is both orthogonal and balanced. Orthogonality refers to the property of a design that ensures that all specified. Minitab was used.

Table 5 Description of Factor Level

Factor Name	***Low Level (mm)***	***Base Level (mm)***	***High Level (mm)***
Length	30	70	80
Space	15	25	50
Depth	10	15	22

According to the design, a 2^3 experimental runs were needed which included 08 experimental runs and simulation, represented in *Table 6*.

Table 6 Two-level Full Factorial DOE

Experiments	***Length (Inch)***	***Space (mm)***	***Depth (mm)***
1	80	50	22
2	30	50	22
3	80	15	22
4	30	15	22
5	80	50	10
6	30	50	10
7	80	15	10
8	30	15	10

The geometrical configuration of all the eight experimental designs are shown in *Figure 14*. The geometrical configuration with the best output values were then considered for a three-dimensional study. In this study we have focused on the two-way ANOVA analysis. Its purpose is to recognize if there is any interaction between dependent and independent variables

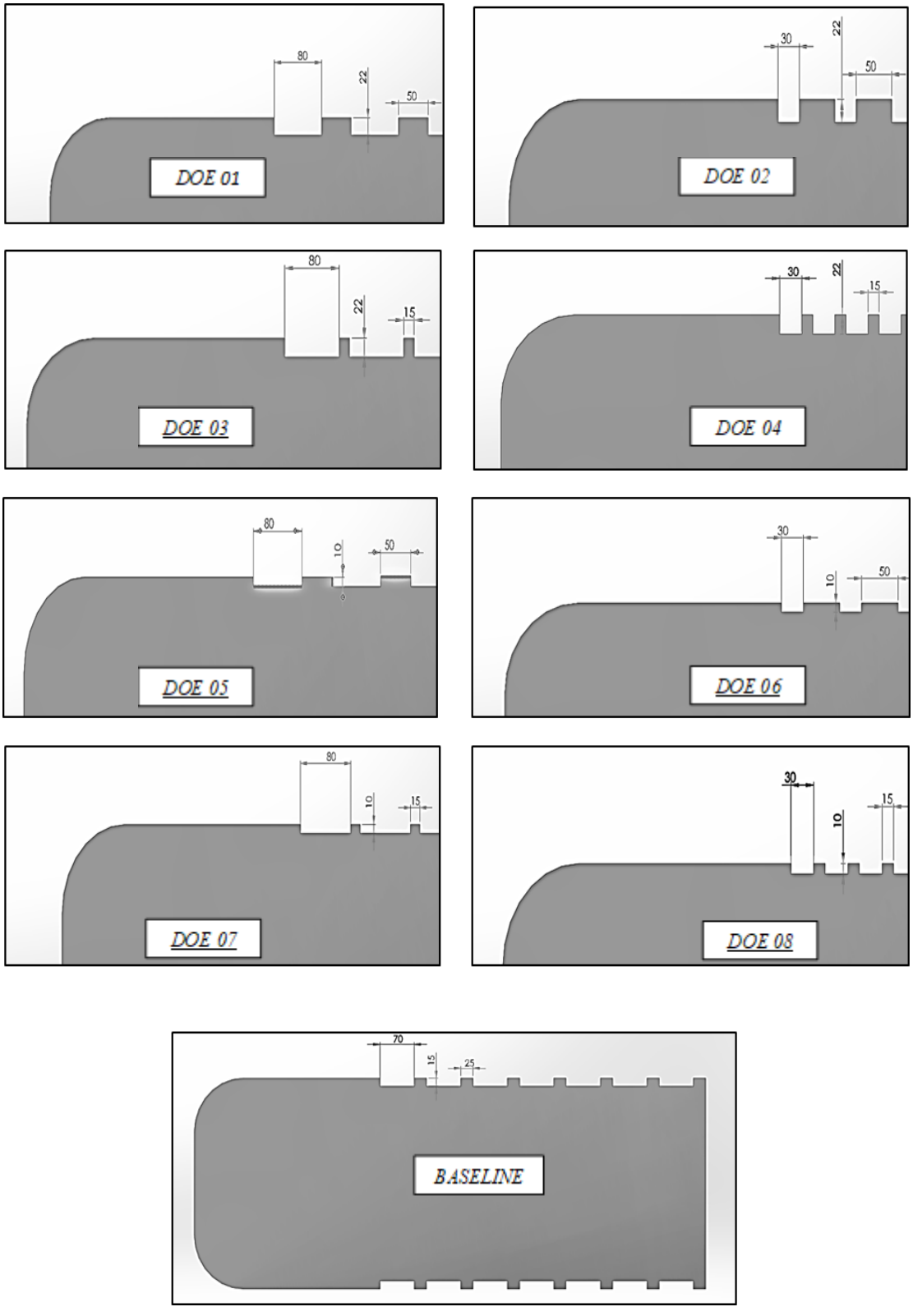

Figure 14 DOE of Ahmed body 2-D

3.3 3-Dimensional Ahmed Body

Huge scope of strategies has been devised to lessen the drag coefficient of a vehicle. In Pakistan, no work has been done to examine the impact of various shapes at the square body of a dumper truck. *Figure 15* shows us couple of types of shapes which are found on almost every dumper truck body.

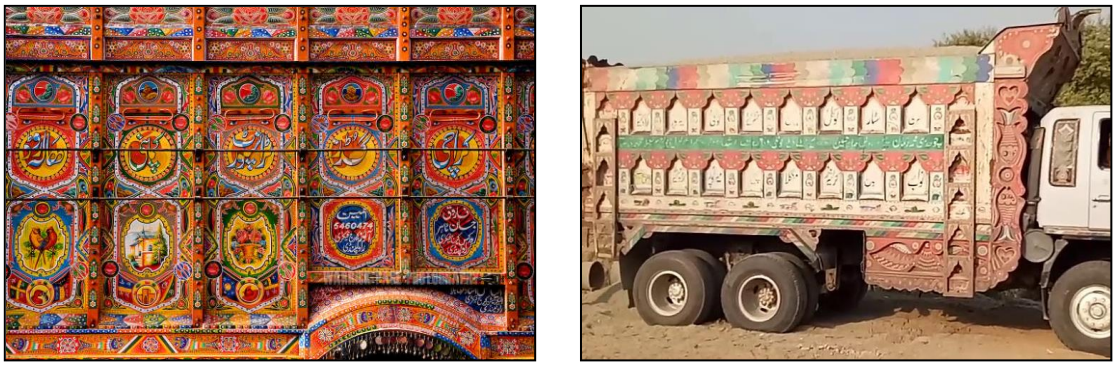

Figure 15 Geometrical shapes at the body of Dumper Truck

A smooth wall square back Ahmed body and two models, one with the lowest and the other with the highest percentage reduction of drag coefficient were selected through DOE for 3-D simulations as show in *Figure 16*. This section describes post and pre-processing of a baseline Ahmed Body, which represent a dumper truck.

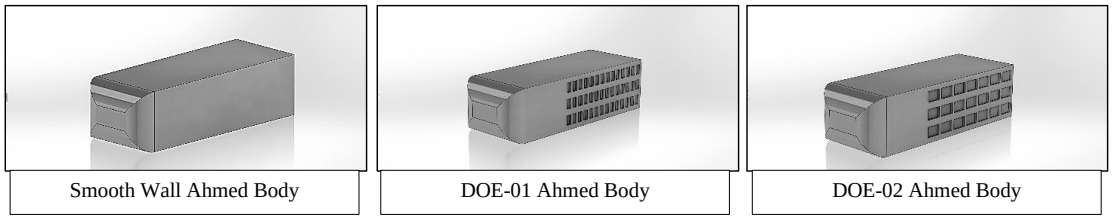

Figure 16 Three-Dimensional Square Back Ahmed Body

3.3.1 Pre-Processing

It is the process that much be performed before doing the actual simulation. It includes, geometrical modelling, computational domain, mesh grid generation and boundary conditions.

3.3.1.1 *Geometrical Modeling*

Figure 9 provides the layout of the geometry of an Ahmed body. Length covered by the slant (L) and its height (H) are calculated below.

$$\cos\theta = \frac{Horizontal\ distance\ covered\ by\ the\ slant\ (L)}{Slant\ length}$$

$$\cos 25 = \frac{L}{222}$$

$$L = 201.2\ mm$$

Therefore

$$x = 1044 - 201.2$$

$$x = 842.8\ mm$$

Also,

$$\sin\theta = \frac{Vertical\ distance\ covered\ by\ the\ slant\ (H)}{Slant\ length}$$

$$\sin 25 = \frac{(H)}{222}$$

$$H = 93.82\ mm$$

Therefore

$$z = 288 - 93.82$$

$$z = 194.18\ mm$$

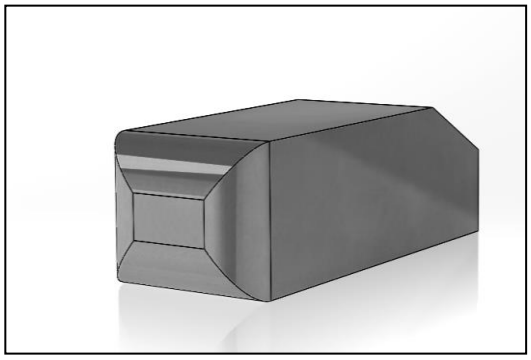

Figure 17 Ahmed body 3D

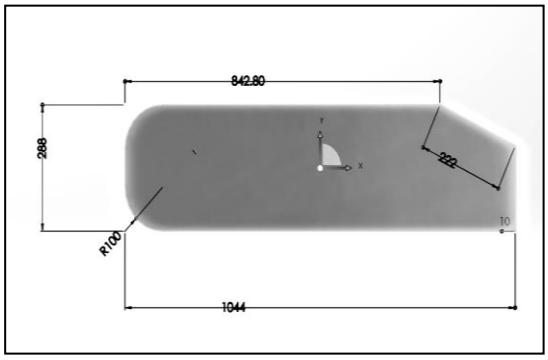

Figure 18 Schematics of 3D Ahmed Body

Figure 17 and *Figure 18* show the schematic and 3-D model of Ahmed body used this this study.

3.3.1.2 *Computational Domain*

The Ahmed body with a length of 1044 mm, 288mm height and a width of 389 mm is placed 50 mm from the ground. The computational domain is created in ANSYS Design Modular and it starts 3500 mm in front of the body, 7956 mm behind, 4000

mm from the top and 3000 mm from the side of the Ahmed body. The computational domain is shown in *Figure 19.*

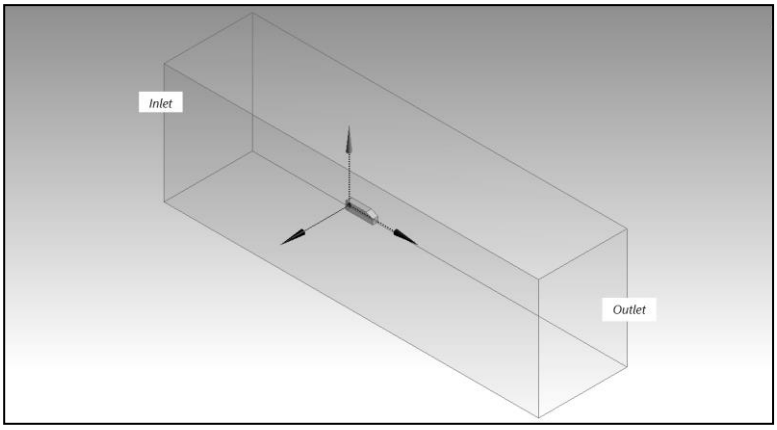

Figure 19 Computation Domain for 3D Ahmed Body

Full model and half model are the two approaches in the software which can be performed for the wind tunnel test. Full model requires the recreation of the whole wind tunnel in the software whereas in a half model only half the object and half the tunnel are modelled. The Ahmed Body and the tunnel are cut along the plane of symmetry offering us with the advantage of less meshing time, a finer mesh and better accuracy.

3.3.1.3 *Mesh Generation*

The surface and volume mesh are generated in ANSYS Meshing. For Ahmed body only surface was created with a total of 1.98 million elements, 15 boundary layers around the body. The mesh is made finer along the surface of Ahmed body to capture smooth transition and gradual increment of mesh was achieved with the appropriate use of growth rate. The distance of first cell away from the surface should be calculated for effective wall shear stress. For that we calculate y^+.

1 *Reynolds Number (R_e):*

$$\mathrm{Re} = \rho v l/\mu$$

$$\mathrm{Re} = \frac{(1.225)(22.22)(0.288)}{1.7894 \times 10^{-5}}$$

$$\mathrm{Re} = 438{,}091.87$$

2 *Skin-Friction Coefficient (C_f):*

$$C_f = [2log_{10}(Re) - 0.65]^{-2.3}$$

$$C_f = [2log_{10}(438091.87) - 0.65]^{-2.3}$$

$$C_f = 4.3519 \times 10^{-3}$$

3 *Wall Shear Stress (τw):*

$$\tau_w = C_f \times \frac{1}{2}\rho U_{freestram}^2$$

$$\tau_w = (4.3519 \times 10^{-3}) \times \frac{1}{2} \times 1.225 \times (22.22)^2$$

$$\tau_w = 1.316\, Pa$$

4 *Friction Velocity:*

$$u^* = \sqrt{\frac{\tau_w}{\rho}}$$

$$u^* = \sqrt{\frac{1.316}{1.225}}$$

$$u^* = 1.306\, m/s$$

For K-Omega models, Y^+=1 is preferred, therefore

5 *Wall Distance (y);*

$$y = \frac{y^+ \mu}{\rho u^*} = \frac{1 \times 1.7894 \times 10^{-5}}{1.255 \times 1.306}$$

$$y = 1.4099 \times 10^{-5} m = 0.014 mm$$

Figure 20 shows the mesh created in our study and in *Figure 21* we can see the prism layers were only present near model boundary where the first layer thickness was 0.014 mm.

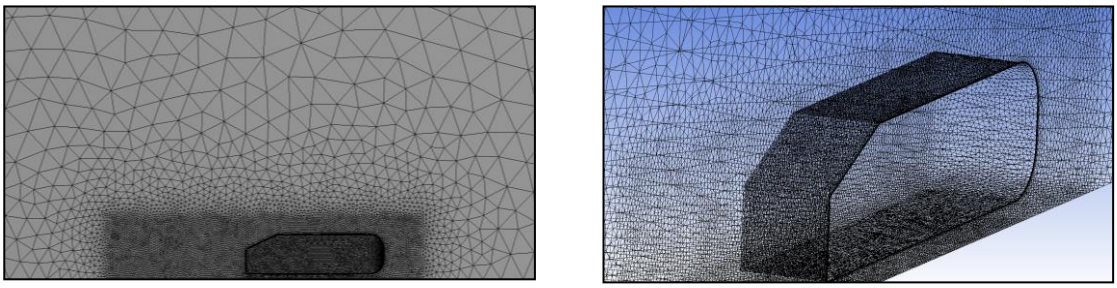

Figure 20 Ahmed Body Mesh 3D

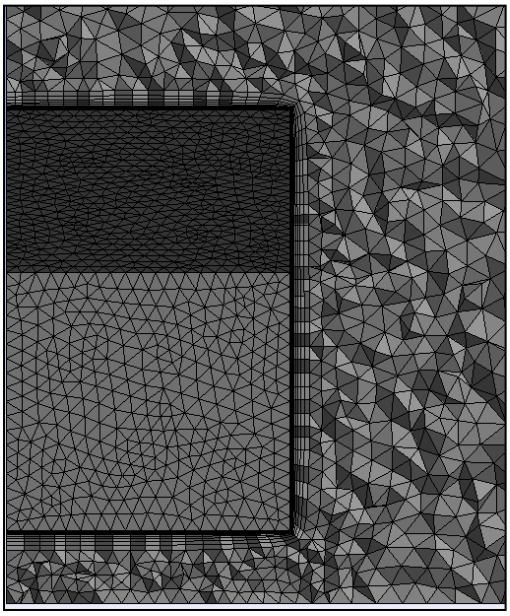

Figure 21 Cut plane along Z-axis showing Prism wall

Grid independence test was undertaken for the Ahmed body and a maximum variation of 10% was found between the coarsest and the finest mesh. The results are shown in *Table 7*.

Table 7 Grid Independence of Ahmed body 3D

Number of Elements	***Coefficient of Drag at 300 iterations (C_d)***
1,448,009	0.2990
1,690844	0.2820
1,981116	0.2698
2,167951	0.2738
2,319848	0.2760

3.3.1.4 *Boundary Conditions*

The model in simulated in pressure-based solver with absolute velocity formulation and time set as transient. A steady state simulation ignores many of the higher order terms dealing with time whereas a transient state does not.

Table 8 Solver Settings

Condition	***Specifications***
CFD Simulation	*3-D Double Precision*
Solver	*Pressure Based*
Velocity Formulation	*Absolute*
Time	*Transient*
Model	*K-omega SST*

K-omega SST model was chosen instead of K-epsilon, with inlet velocity of 22.22 m/s. This is because k-omega and RSM are more accurate that k-epsilon in situation where flow is more linear (k-omega) or more complex (RSM). K-omega is particularly the best option where the flow is near the wall regions, such as ours where RSM requires a very high cell mesh to provide accurate results. Turbulent intensity for inlet turbulence was set to 1% for velocity because the air is going to be a lot calm at the inlet. For pressure outlet we set the turbulent intensity to 5% because after the flow has encountered an obstacle, Ahmed Body in our case.

Pressure based COUPLE solver is used as a solution method. Second Order Upwind was kept for momentum, turbulent kinetic energy, and specific dissipation rate to achieve more accurate results. 0.25 relaxation factor is used for both momentum and pressure in this study and the turbulent viscosity is dropped to 0.9.

Under solution limits, the maximum turbulent viscosity ratio is increased from $10e^{+4}$ to $10e^{+6}$ to avoid the possibility of a warning message after every iteration that the maximum turbulent viscosity ratio was limited to a certain cell number. It does not affect the solution in any way. For our domain to show realistic distribution of pressure and velocity we opted hybrid initialization

3.4 Pakistani Dumper Truck

In the last phase eight times scaled down model of an original Pakistani Dumper Truck was developed *Figure 22*. It was considered as a model of reference. Out of the two DOE models that were selected for 3-D Ahmed body study, only one was chosen

whose groove configuration was modeled on Pakistani dumper truck without any add-on devices (*Figure 23*) . Add-on devices such as front fairing (*Figure 25*) and side extenders (*Figure 24*) were also modeled on the Pakistani dumper truck along with the selected square groove geometry and the results were compared with the baseline model.

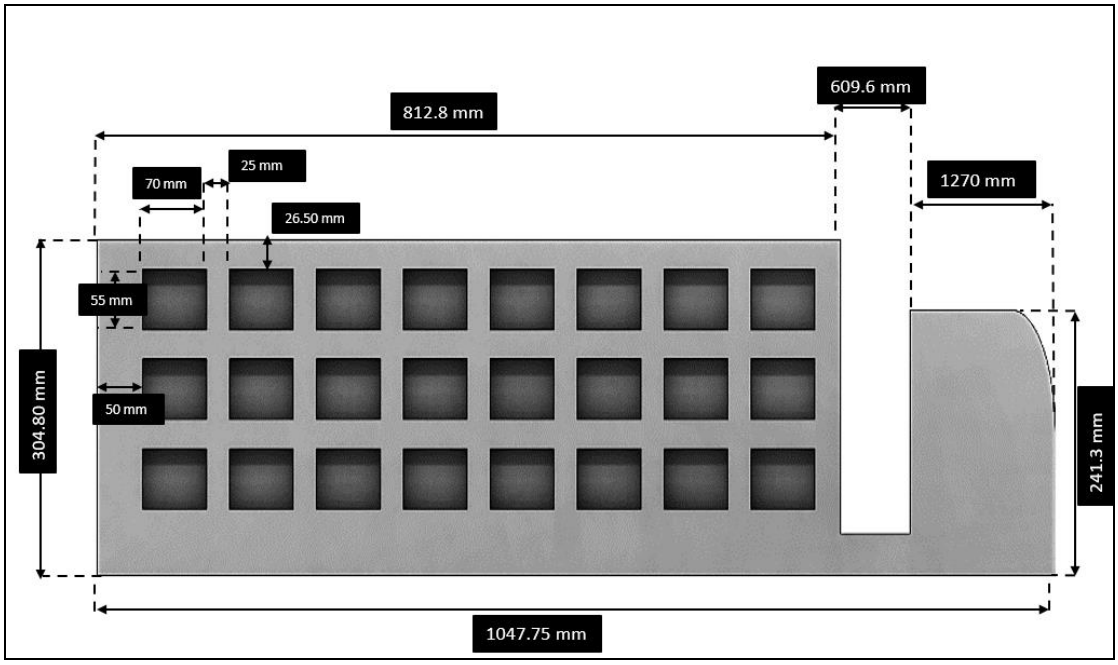

Figure 22 Baseline Pakistani Dumper Truck

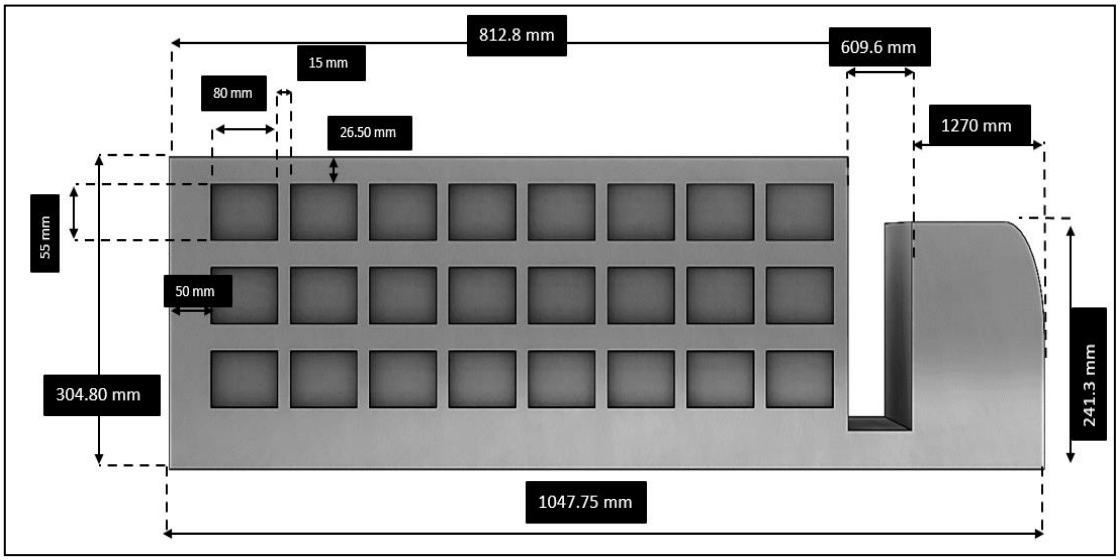

Figure 23 Dumper Truck with Optimized Grooves

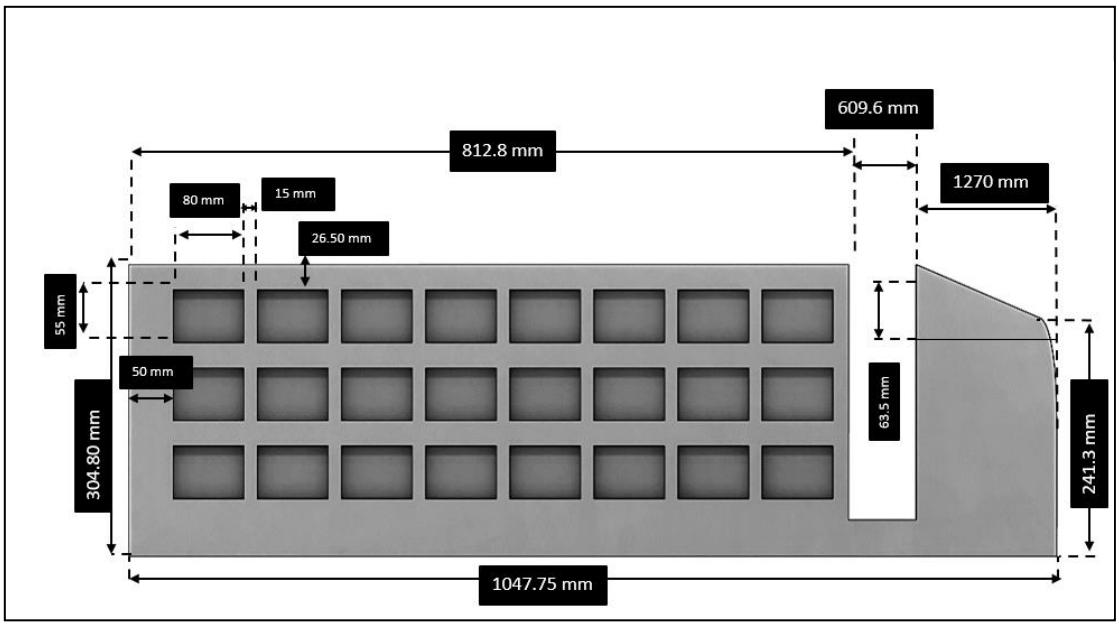

Figure 25 Dumper Truck with Optimized Grooves and Front Fairing

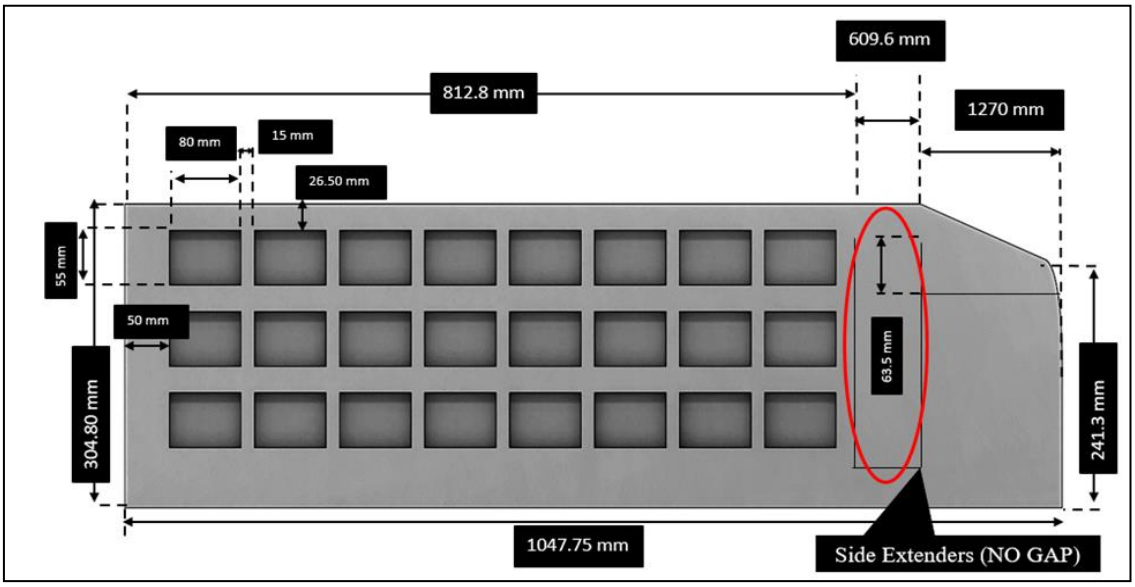

Figure 24 Dumper Truck with Optimized Grooves, Front Fairing and Side Extenders

3.4.1 CFD Model Validation

Ahmed body is widely used for the validating new model of road vehicles. It was first proposed by Ahmed in 1984 [3] in which the body was placed in a wind tunnel and the flow structure around the body causing wake was analyzed. 85 percent of the drag was credited to pressure drag and its dependency on the slant angle was uncovered.

Wind tunnel testing was not performed for this study because of the lack of equipment and because it takes a lot of time for developing a scale model. Flow inside a low

quality or a small tunnel can also be affected due to tunnel walls which leaves us with CFD which, in comparison, is both cost and time effective with better visualization of results.

The mesh around the body is shown in *Figure 20* and the simulation was run at 22.22 m/s with first layer boundary thickness of 0.014 mm with 1.98 million number of elements. The resultant flow, through velocity streamlines, of the simulation is shown in *Figure 26*.

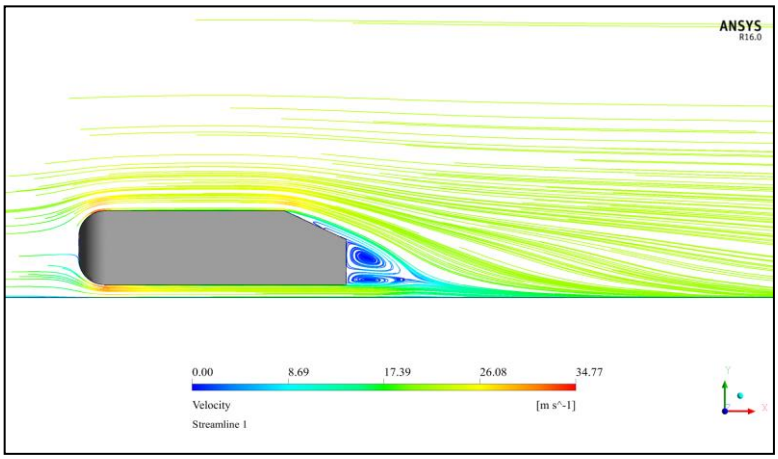

Figure 26 Flow around Ahmed Body Velocity Contour

Drag coefficient value of experimental studies from literature and our simulation are compared in *Table 9*.

Table 9 Drag Coefficients for Ahmed Body

Model	***Coefficient of Drag (C_d)***
Ahmed 1984	0.280
ANSYS Fluent	0.278

These results prove strong evidence for the validity and accuracy of the results obtained from the simulation.

3.5 Summery

First the flow movement inside the transverse grooves were simulated using a flat plate. The same technique was shifted to test the flow in a 2-Dimensional Square back Ahmed Body, which in this case was considered as a Dumper Truck. After its hopeful results, DOE was performed to achieve drag coefficients trends when modifications were done in the geometry of the square grooves. Finally, the design with the best drag coefficient was modeled in in 3D along with the validation from experimental studies in literature of a basic Ahmed body.

3.6 Reference

[1] C.-H. Bruneau, I. Mortazavi, and P. Gilliéron, "Passive Control Around the Two-Dimensional Square Back Ahmed Body Using Porous Devices," *J. Fluids Eng.*, vol. 130, no. 6, p. 061101, 2008.

[2] G. Schewe, "Reynolds-number effects in flow around more-or-less bluff bodies," *J. Wind Eng. Ind. Aerodyn.*, vol. 89, no. 14–15, pp. 1267–1289, 2001.

[3] A. S, "Some Salient Features of the time-Averaged Ground Vehicle Wake," *SAE*, 1984.

Chapter 4: Results and Discussions

The simulations performed during this study are explained in this chapter. This research was carried out in various steps so that optimum solution can be derived. Keeping this motivation, simulations were performed firstly on a flat plate with and without a square groove. Following this, DOE was carried out and simulations based on 8 different configurations were performed on the 2-D Ahmed body. This was done to verify if it has any effect on the wake so that time and effort can be saved before performing it on 3-D Ahmed body if no difference is observed. After this experimentation 2 best configuration were selected and used on 3-D Ahmed body with square back.

A 3-D of dumper truck was modelled for the experiment so to notice any changes that appear in the flow of air. The configuration giving best results on the previously performed simulation on 3-D Ahmed body with square back was selected for 3-D dumper truck. CFD simulation using add-on devices such as front fairing and side extenders were also performed on dumper truck to study their effects on the drag coefficient.

4.1 Flat Plate

Graph 2 explains and validated through literature that there is a sharp rise in skin friction coefficient immediately before and after the grove. The stagnation edge downstream of the groove gives rise to a favorable pressure gradient hence the overshoot.

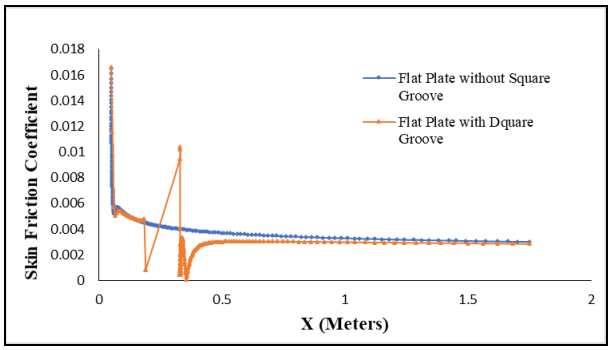

Graph 2 Skin Friction Coefficient: Flat Plate VS Grooved Plate

The skin friction coefficient gradually decreases. After that, the undershoot on the graph indicates us that because of change in no-slip condition the flow tries to recover. The skin friction coefficient that oscillates back to the smooth value This in turn modifies the near-wall activities responsible for momentum change and turbulent skin friction.

In *Figure 27*, a) and b) show the velocity contours of a flat plate with and without a square groove. The results in figure c) reveals that a separation bubble is generated inside the square groove transform the laminar boundary layer into turbulent. The flow separates upstream of the groove and then reattaches downstream of the groove causing the formation of separation bubble. This leads to a pressure difference, as a

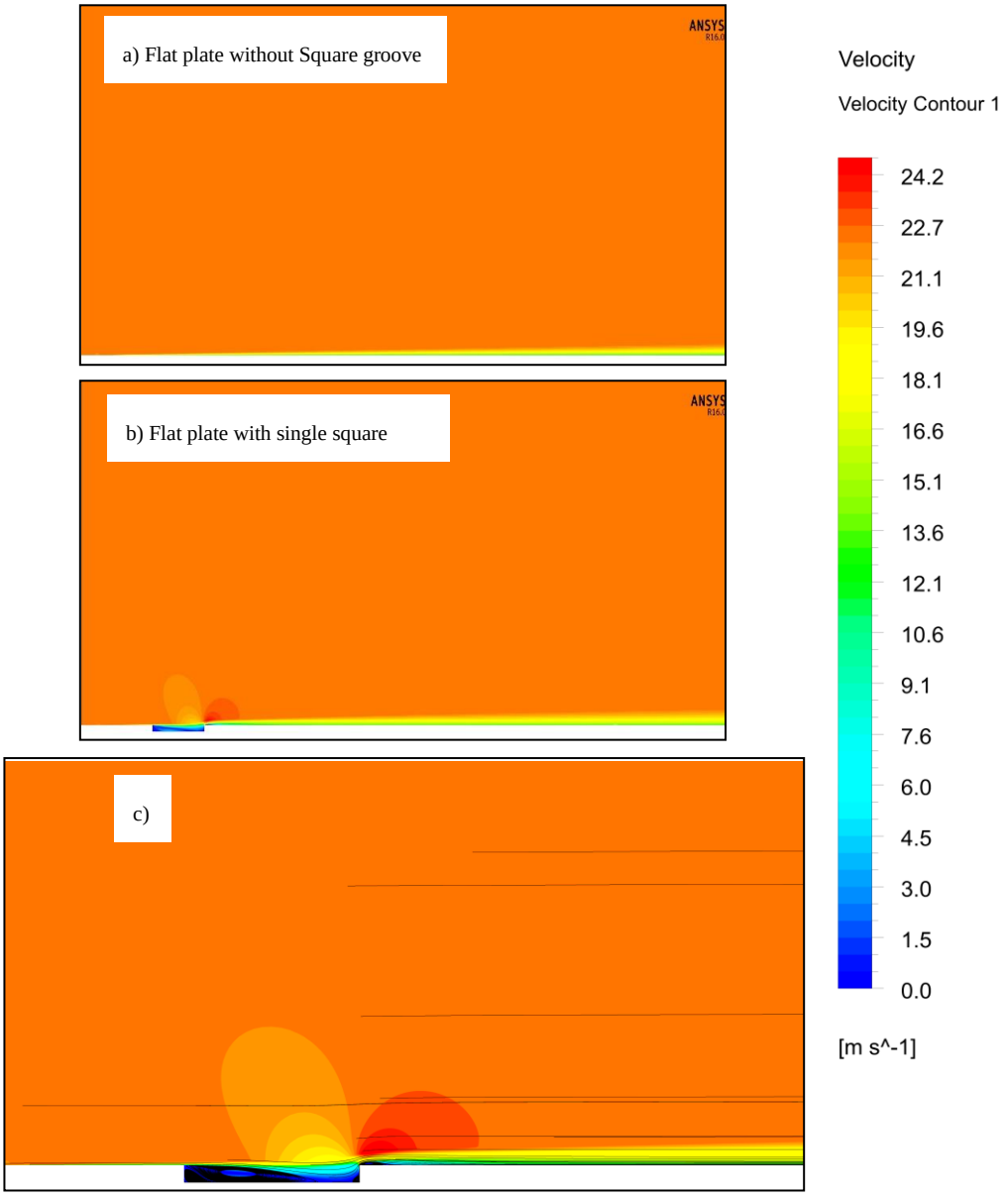

*Figure 27 Velocity Contour: **a)** Flat Plate **b)** Flat Plate with Single Square Groove **c)** Closeup of Square Groove with Streamlines*

low-speed flow circulates inside the groove

4.2 Ahmed Body (2-Dimensional)

The key reason for using a non-smooth, grooved surface is to facilitate a turbulent boundary layer which may result in delayed separation of the flow resulting in a smaller wake and a lower drag.

Square grooves cause an increase surface roughness as witnessed in the case of flat plate with a square groove. The skin friction component of total drag gets intensified. In case of an Ahmed body, which is considered as a buff body like dumper trucks, the component of form drag is more dominant as compared to drag due to skin friction.

From *Figure 28* we can see that there are two major regions of low velocity i.e. less than 22.22 m/s. The first one is just before the front face of the body which is due to the stagnation of the flow as it demonstrates more air resistance. The flow intensity dwindles as the flow starts gliding over the square grooves. The second is just downstream of the body. Finally, the flow streamlines meet further downstream which is why a steady change in the flow velocity can be seen.

In *Figure 28,* from DOE 01-08 it is found that by incorporating square grooves, while most of the wake structure was more or less similar, the air flow distributions were differently marked. The drag is reduced as the turbulent boundary layer is developed which has a greater momentum hence shifting the separation point.

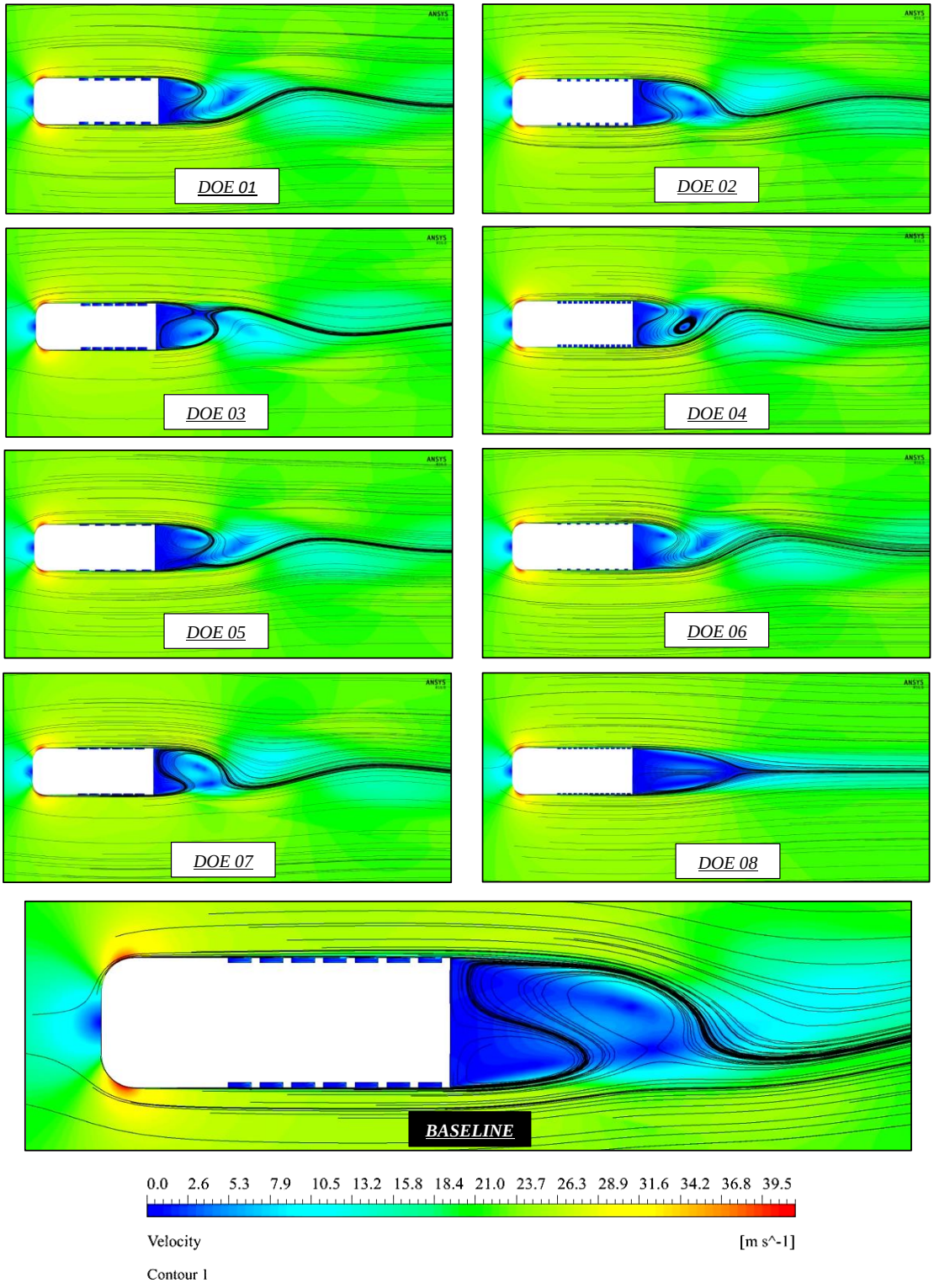

Figure 28 Velocity Contours of the Baseline model and Eight Different Configuration of Ahmed Body used in DOE

A strong negative pressure zone can be seen behind the Ahmed body. As evident from the *Figure 29* that in all the models of square back Ahmed body the pressure contours hold their general pattern all over. When the air flows around the body, the

pressure begins to drop which increases the velocity of the air flow as it moves over the square grooves.

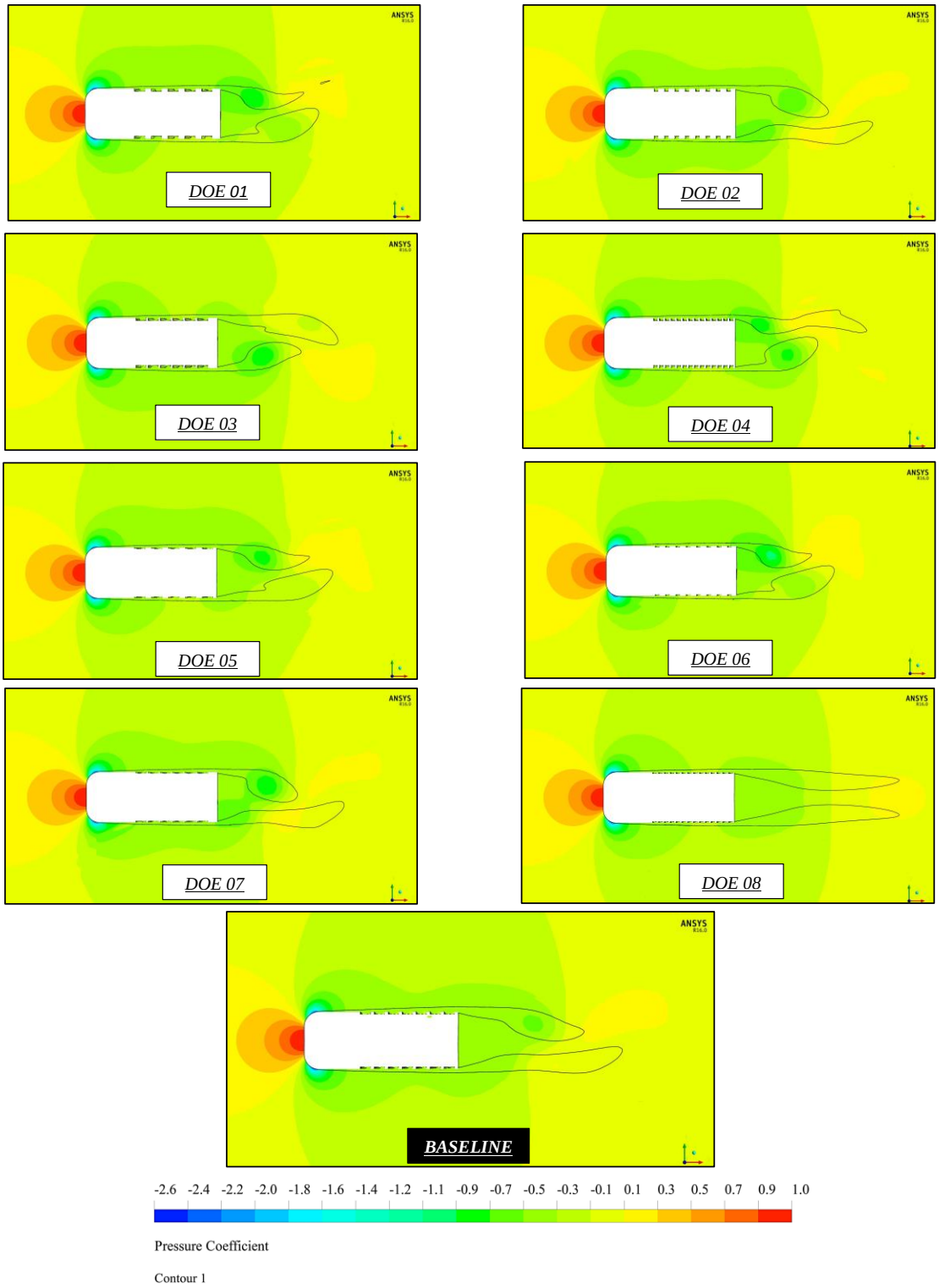

Figure 29 Pressure Contours of the Baseline model and Eight Different Configuration of Ahmed Body used in DOE

The results from the CFD simulations indicate that the baseline model produced a drag coefficient of Cd = 0.321. DOE approach was employed to create surrogate models and these models were used to determine the sensitivity of the design variables.

A DOE with 2 levels and three factors was chosen for a full factorial. The whole experimental plan included 08 experimental runs. The model data base is constructed using Minitab and CFD simulations are carried out for every model. The choice of computational set up was kept the same for all the models. The simulation results are shown in *Table 10*.

Table 10 Results of Two-level Full Factorial DOE

Experiments	***Length (in)***	***Space (in)***	***Depth (in)***	***Coefficient of Drag (C_d)***	***Percentage Drag Reduction***
1	80	50	22	0.306	4.6%
2	30	50	22	0.300	6.5%
3	80	15	22	0.304	5.3%
4	30	15	22	0.301	6.2%
5	80	50	10	0.300	6.5%
6	30	50	10	0.302	5.9%
7	80	15	10	0.301	6.2%
8	30	15	10	0.315	1.9%

In this study we have focused on the two-way ANOVA analysis. The results displayed in the *Table 10* show that the drag coefficient can be decreased significantly by all options: the smallest reduction is 1.9% and the largest reduction being 6.5%.

In *Figure 30* we look to see if the lines are parallel or not. If they are not parallel it means that our independent variables, length space and depth of the groove, are interacting with each other. In other words, they are creating a specific combined effect on our output to get something that we would not get doing it separately.

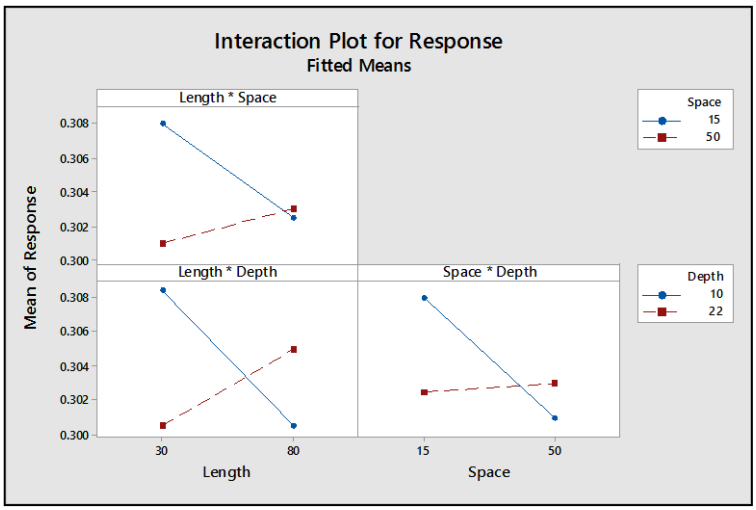

Figure 30 Interaction Plot for Response

Different slopes suggest that interaction might be present. The first graph in the upper left corner in *Figure 30* is an interaction between length of the groove and the space between two grooves. It shows that the model with lower levels of space and length factor, yields higher drag coefficient. The model with lower factor level of spacing between the grooves and a higher lever factor of length yielded almost similar results as the model with higher factor level of space and length of the groove. Ahmed body with higher factor level of space and lower factor of length generated the lowest drag coefficient.

Second graph at bottom left show the interaction between length and depth factors of the groove. It reveals that the model with the lower factor levels of depth and length results in the highest drag coefficient. The lowest drag coefficient is achieved by a lower depth factor and a higher length factor, as well as by setting higher depth and lower length factor. Whereas the setup of higher depth and length factor resulted in a slightly above the mean drag coefficient.

The third and the final graph in this figure displays the interaction between the space and depth of the groove. It uncovers that the model with the lower factor levels of space and depth results in the highest drag coefficient. The higher depth factor and lower space factor yielded almost the same drag coefficient as did the model with higher factor of depth and space. However, the model configuration with lower depth and higher level of space factor resulted in the lowest drag coefficient.

Figure 31 tells us that as we approach to the higher level of all three factors the drag coefficient decreases. Space being the most prominent factor in controlling the drag behind the Ahmed body with a square back. It shows that the space and length factor has the most significant effect on drag coefficient.

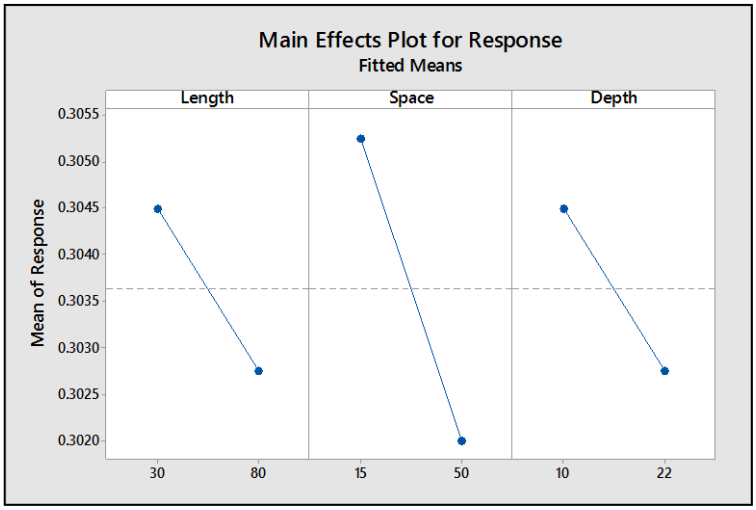

Figure 31 Main Effects Plot for Response

4.3 3-Dimensional Simulations

4.3.1 Ahmed Body with Square Back

This segment describes the flow structure around the Ahmed Body and its wake. Three simulation were performed. The first one is of a smooth surface square back Ahmed body and the other two simulations were performed on the models that yielded the highest (DOE-08) and lowest drag coefficient (DOE-07) during the 2-dimensional DOE. All simulations were carried out under the same grid and boundary conditions.

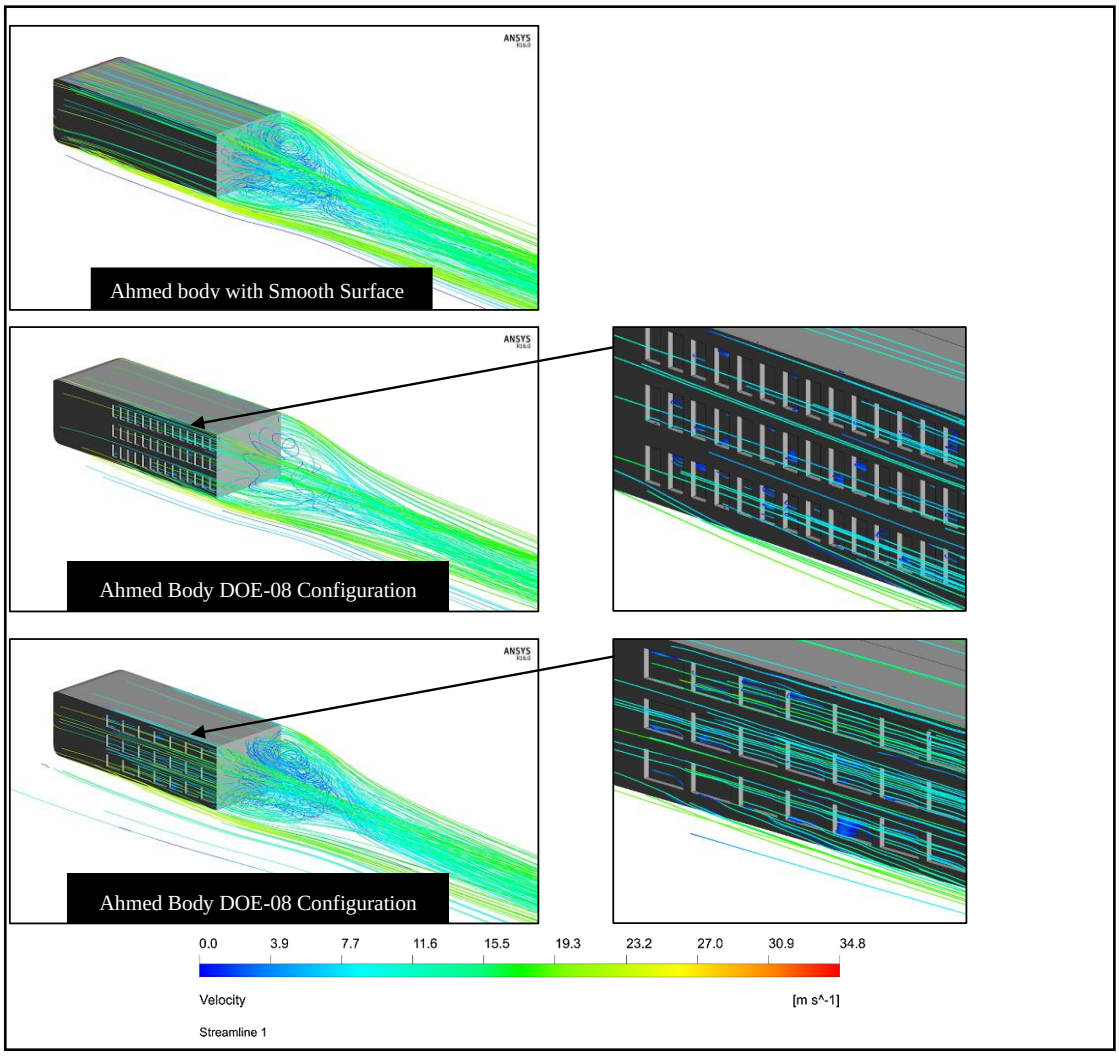

Figure 32 Velocity Streamline on Square Back Ahmed Body with Different Groove Configurations

Velocity streamlines around three different configuration of Ahmed body are presented in *Figure 32*. The figure above tells us that in the case of model DOE-08, groove geometry with a shorter length, the flow entering the number of grooves as well as the amount of flow entering a single groove is almost negligible as compared to the model DOE-07 which has a larger groove length.

From the *Figure 32* we can conclude the flow velocity between the grooves is greater than that of inside it. Ahmed body has a turbulent flow transition as the flow enters the groove creating a small separation bubble, upstream of the groove, hence accelerating the flow between the grooves on Ahmed body's surface. The low velocity circulation of the flow results in a pressure difference between the groove and body surface. In the case of a grooved Ahmed Body the adverse pressure gradient can overpowered by such a flow pattern, allowing us to control the boundary layer thickness.

The results from the CFD simulations are presented in the *Table 11* show that the Ahmed body model with DOE-07 configuration resulted in a decrease of 3.17% which can also be seen in *Figure 32* as the wake structure starts to change and the flow starts to reach at the back of the body in DOE-08 model.

Table 11 Drag Coefficients for 3-D Square Back Ahmed Body

Serial No.	***Model***	***Drag Coefficient***	***Percentage Difference***
1	Smooth Wall	0.284	-
2	DOE-08	0.282	0.70%
3	DOE-07	0.275	3.17%

Pressure and turbulent kinetic energy distribution at iso-surface at X=200 mm shown

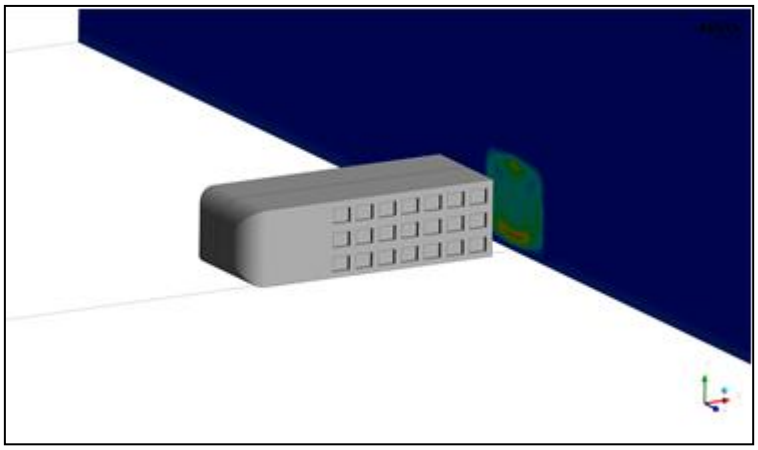

Figure 33 Iso-Surface at X=200 mm

in *Figure 33* and are presented in *Figure 34* and *Figure 35.*

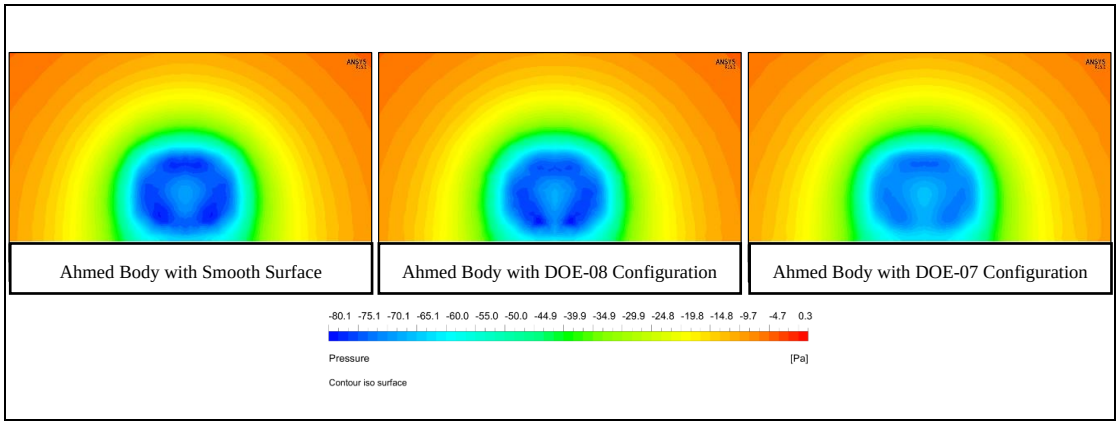

Figure 34 Iso-Surface Pressure Contour at X=0.2m

Pressure contour in *Figure 34* indicate that the negative pressure zone of the wake decreases after the square grooves were added to the surface. The negative pressure zone was minimal for model DOE-07 compared to the other two.

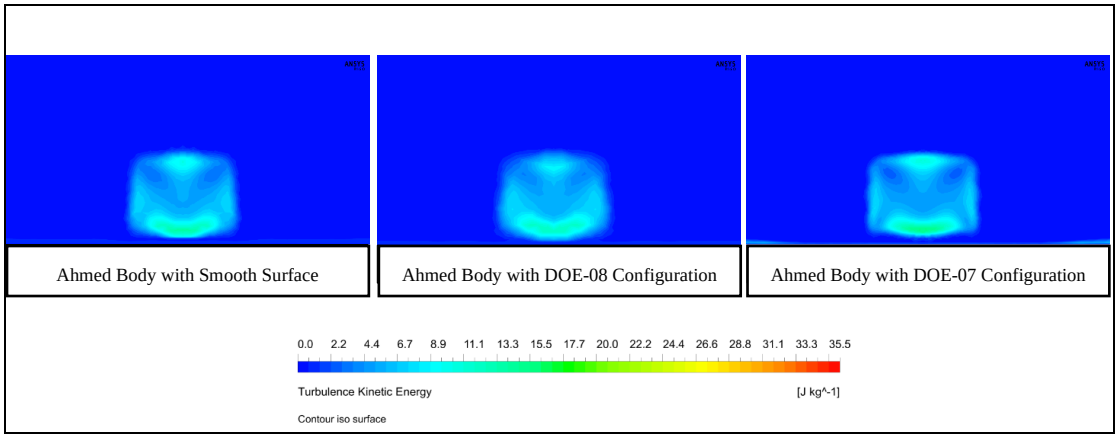

Figure 35 Iso-Surface Turbulent Kinetic Energy Contour at X=0.2m

Figure 35 demonstrates the three-model relation. The model DOE-07 shows the highest turbulent fluctuation while the model DOE-08 has the lowest turbulent fluctuation. The added momentum by the grooves to the flow near the boundary layer can be seen by the increased turbulent fluctuations. This implies that once the grooves were added to the surface, the energy dissipation decreased. With the extra energy the flow gets further down the body until the seperation takes place.

4.4 Pakistani Dumper Truck

For the scaled down dumper truck the simulations performed were with the same pre-processing including computational domain, grid, boundary condition etc. as were in the case of Ahmed body

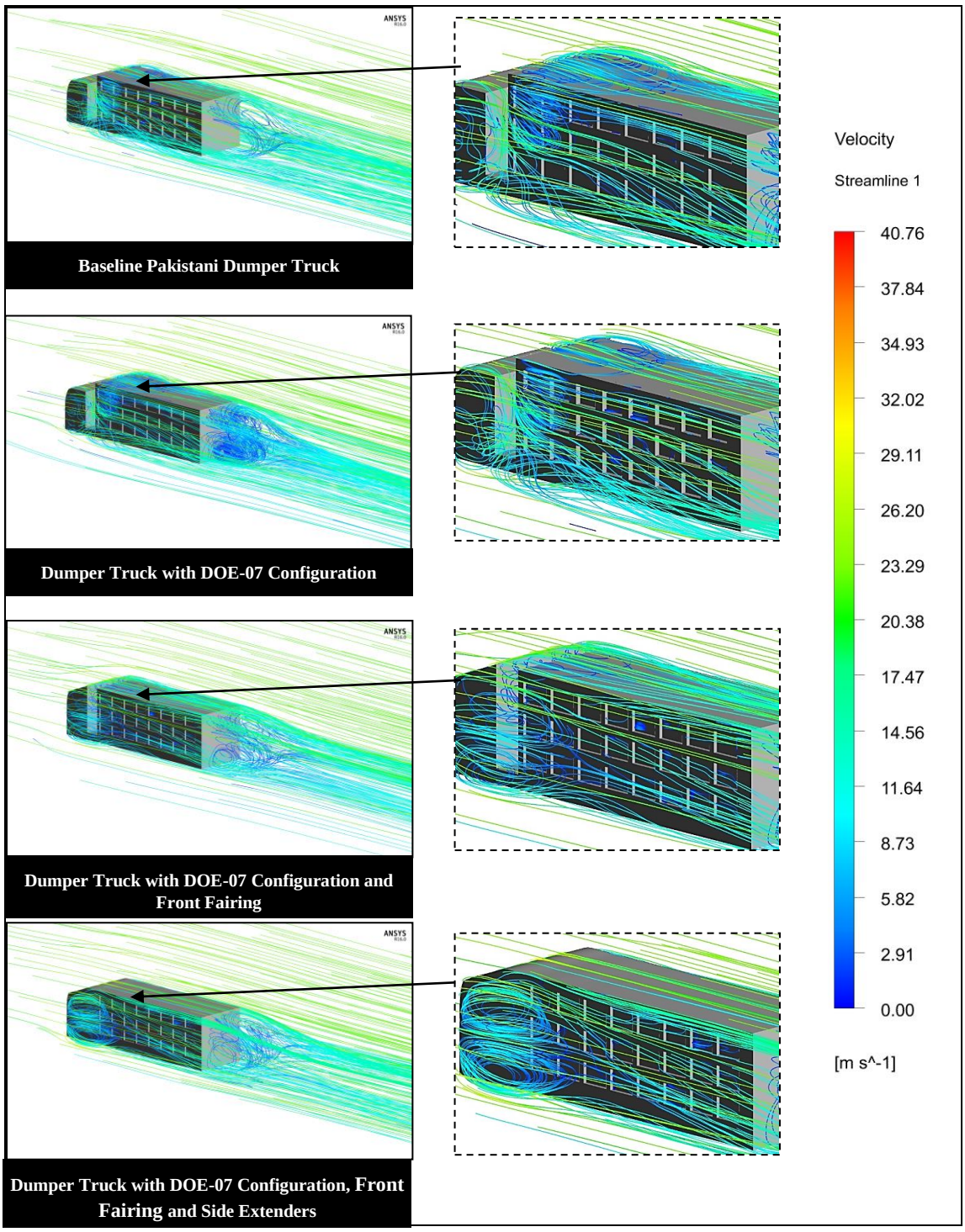

Figure 36 Velocity Streamline of Baseline Dumper Truck with Optimized Grooves and Add-on Devices

Velocity streamline are presented around the baseline Pakistani dumper truck and its three different configurations in *Figure 36* . In the case of baseline Pakistani truck, the air flow around the dump bed and its circulation between the gap is almost the same as in the case of dumper truck with DOE-7 design (optimized) square grooves. Baseline and optimized groove model yield drag coefficient 0.825 and 0.829 respectively, which shows no significant. The air flow distributions were differently marked.

For the case of dumper truck with DOE-07 design and front fairing, the air flow inside the grooves is evident from the figure above. Hence, resulting in creating a small separation bubble upstream of the grooves and therefore accelerating the flow between the grooves just like in the case of grooved Ahmed body. This resulted in a 26.3 percent decrease, yielding a drag coefficient of 0.608.

For the last case, DOE-07 design grooves with front fairing and side extenders, the air flow along the model is almost the same as in the case of previous model with front fairing. What counts is the is the velocity of the air flow around the dump. Despite having similar flow structure, the velocity of the flow in case of the side extenders is higher than the front fairing truck which is an indication of pressure drop. As there is no gap between the dump bed and driver's cabin, there is no adverse pressure gradient to overcome and the flow tends to stay connected for a longer distance along the body, allowing it to reach the back and reducing the wake. The model generates a drag coefficient of 0.587 causing a 4.44 percent decrease from the front fairing model.

Table 12 Drag Coefficient of Pakistani Dumper Truck with Different Configuration and Add-on Devices

Serial No.	***Model***	***Drag Coefficient***	***Percentage Reduction from Baseline***
1	Baseline Pakistani Dumper truck	0.829	-
2	Dumper Truck with DOE-07 Configuration	0.825	0.48%
3	Dumper Truck with DOE-07 Configuration and Front Fairing	0.608	26.65%
4	Dumper Truck with DOE-07 Configuration, Front Fairing and Side Extenders	0.587	29.19%

The outcomes from the CFD simulations are presented in the *Table 12* show that the dumper truck with DOE-07 groove design with front fairing and side extenders resulted in a cumulative decrease of 29.19% from the baseline model. Whereas the dumper model with DOE-07 groove design and front fairing caused a reduction of 26.65% from the baseline model and the model with only DOE-07 groove design resulted in 0.48% reduction.

Similar approach for pressure and turbulent kinetic energy distribution on iso-surface in the case of Ahmed body has been adapted for dumper truck models.

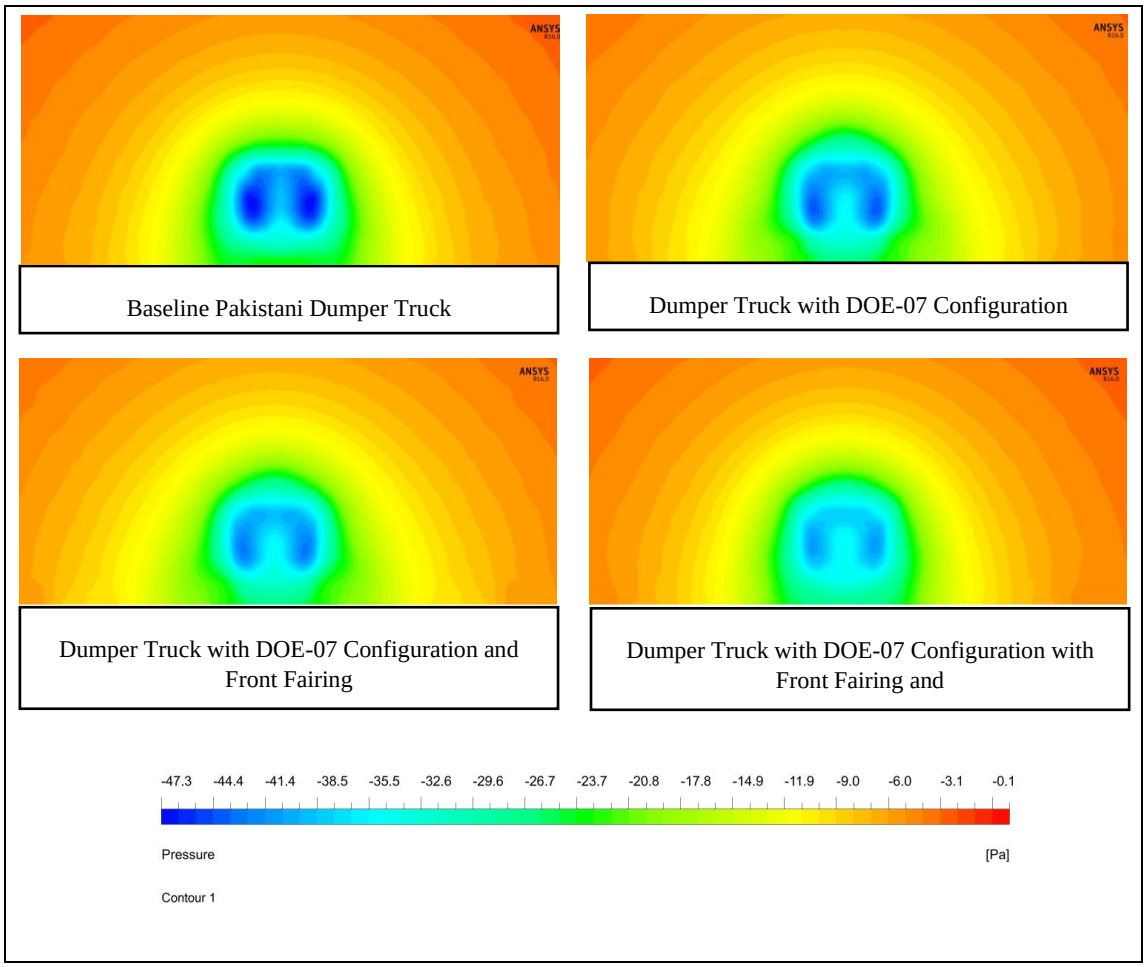

Figure 37 Iso-Surface Pressure Contour at X=0.2m

Pressure contour in *Figure 37* show that the negative pressure zone of the wake decrease after the DOE-07 configuration grooves employed on the baseline Pakistani dumper truck. The negative pressure zone further decreases in the case DOE-07 model with front fairing and is found to be the smallest for that last model with DOE-07 configuration, front faring and side extender.

Figure 38 demonstrates four-model relation. The baseline Pakistani dumper truck shows the highest turbulent fluctuation while the model with DOE-07 configuration displays comparatively less turbulent flictuation which are almost insignificant. The increase in turbulent fluctuation becomes the most prominent in the third model with DOE-07 configuration and front fairing. For the last model with DOE-07 configuration with front fairing and side extenders the trubulent fluctuation is very low in comparision with the first two models. Relative to model with front fairing, the trubulent fluctuations at the top back of the side extender model is greater.

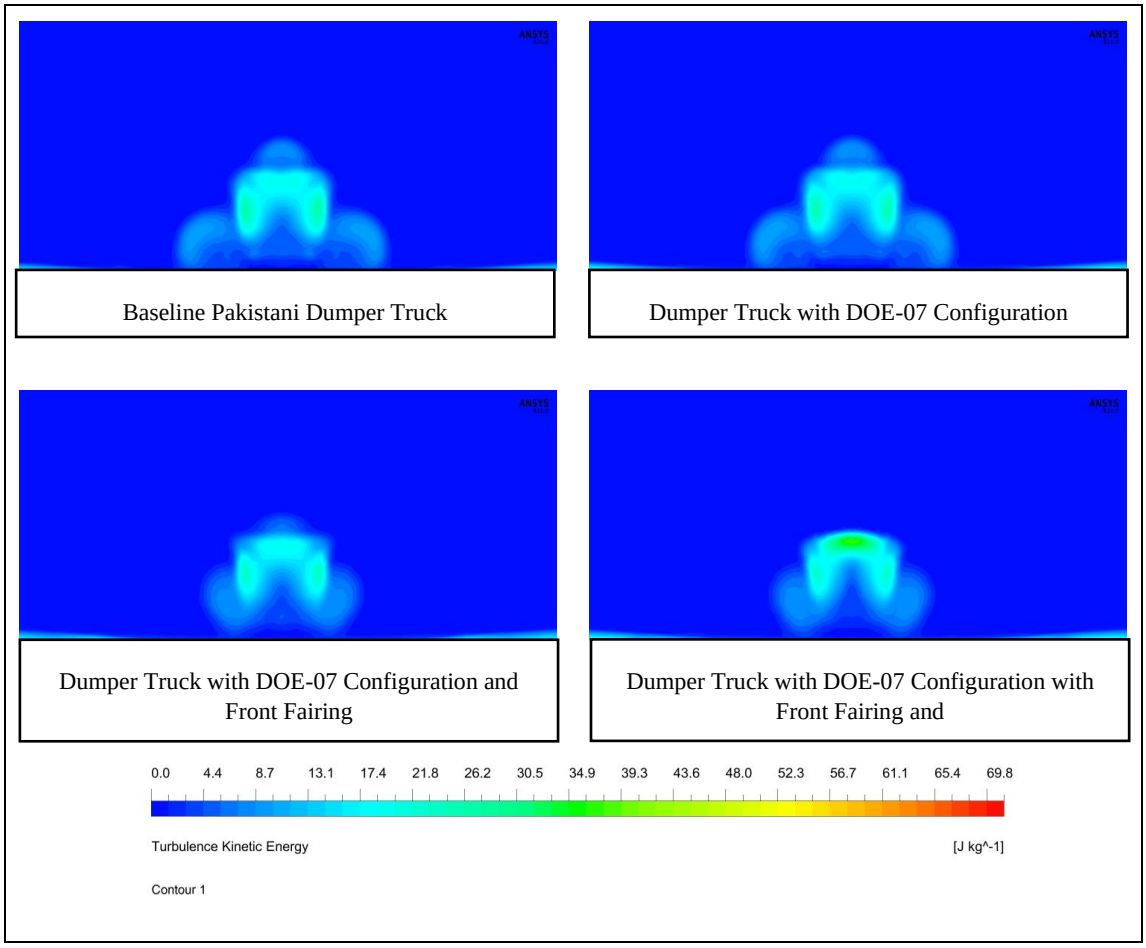

Figure 38 Iso-Surface Turbulent Kinetic Energy Contour at X=0.2m

4.5 Summary

The passage of quasi-streamwise vortices is responsible for the interaction between the groove and the outer flow. This in turn modifies the near-wall activities responsible for momentum change and turbulent skin friction.

For all these eight 2-dimensional models with different groove configurations the air flow distribution is different whereas wake structure is more or less the same. Grooves cause a turbulent boundary layer on the surface which has greater momentum than the laminar boundary layer, causing a delay in separation.

In the case of 3-dimensional models negative pressure zone of the wake decreases after the grooves are added of the Ahmed body. Model with DOE-07 configuration had the minimal negative pressure zone.

Finally, for the dumper truck, model with front fairing and side extenders has the smallest negative zone

Chapter 5: Conclusion

This chapter summarizes the findings extracted from the whole study. This thesis is aimed mainly at finding out that whether square grooves, that are found on every truck body in Pakistan, help is shaping the aerodynamics of the air flow aroud its body by delaying the seperation point or not. And to achieve the best geometrical configuration of the square grooves in case they had any impact on the wake of the body.

5.1 Conclusions:

I. Air flow over the square groove results in the formation of a separation bubble inside it. This gives rise to a pressure difference since the separation bubble causes low velocity circulation flow. Resulting in increased skin friction coefficient. This in turn modifies the near-wall activities which are responsible for momentum change.

II. By the means of DOE, eight different configurations of the baseline groove found on the dumper truck are established to determine the sensitivity of the design. The baseline model produced a drag coefficient of 0.321.

III. After simulating all eight DOE model on a 2-dimensional square back Ahmed body, two configurations were selected. Most of the wake structure was more or less similar but the air flow distributions wee marked differently. The smallest reduction was 1.9% and 6.5% being the largest.

IV. Model configuration of DOE-07 and 08 were selected for 3-dimensional simulations as they yielded the lowest and largest drag coefficient, respectively. DOE-07 configuration resulted in a 3.17% of drag reduction whereas the other only reduced 0.70% drag coefficient. Therefore, concluding that the length of the groove has a more prominent effect on the wake of the body as compared to spacing between the grooves and its depth.

V. DOE-07 configuration was then employed on a scaled down Pakistani dumper truck and as a result C_d dropped from 0.829 to 0.825, as compared to the baseline truck, causing a 0.48% reduction in drag.

VI. Different add-on devices were tested on the dumper truck model with DOE-07 configuration. The one with the front fairing cased a 26.65% decrease in drag coefficient, when compared with the baseline dumper truck.

VII. With the addition of side extenders to the front fairing model the drag coefficient further reduced to 29.19%

5.2 Recommendations for Future Work:

In this this all the focus was on the groove geometry whereas there are also other crucial aspects that can affect the drag coefficient. Further improvements can also be made that include:

I. Instead of keeping the rear of the body flat, a boat-tail like structure can be used.

II. Investigating the under-body effect, which was not done due to computational limitations.

III. Performing simulations on different yaw-angles.

IV. Applying DOE on the geometrical configuration of front faring.

V. Conduction an experiment using a wind tunnel for more realistic visualization.

Appendix

ICRANET2018- 180513

COMPUTATIONAL INVESTIGATION OF DRAG REDUCTION ON AN AHMED BODY USING SQUARE GROOVES

Rawail Haseem
Department of Thermal Energy Engineering
National University of Sciences and Technology, NUST
H-12 Main Campus, Islamabad
rawail_haseem@hotmail.com

Adeel Javed
Department of Thermal Energy Engineering
National University of Sciences and Technology, NUST
H-12 Main Campus, Islamabad
adeeljaved@uspcase.nust.edu.pk

Abstract
In Pakistan 96% of the freight transportation is done through trucks[1]. This aerodynamic pressure drag causes up to 15-20% extra fuel consumption [2]. Aerodynamic drag can be reduced by using different passive techniques of fluid flow control. In this paper, the influence of square grooves on the passive drag reduction has been evaluated. In the first phase simulations have been performed to investigate the skin friction coefficient of smooth flat plate with square groove in it. These grooves are placed transverse to the incoming flow. This results in increasing the friction drag along the boundary causing the transition of laminar flow to turbulent. Similar technique is used in the second phase around a square back Ahmed Body. The study has been conducted with computational fluid dynamics (CFD) simulations using ANSYS Fluent. Unsteady Reynolds Averaged Navier-Stokes (URANS) formulation has been employed with Transient time and 2 equation k-epsilon realizable model, in the simulation. The focus of this study is to help the transportation sector of Pakistan by making efficient aerodynamic design. This study is applicable to Pakistani heavy transport vehicles with an intention to reduce the high fuel consumption which is caused due to high pressure drag

Keywords: Ahmed Body; CFD; Flat Plate; Square Grooves.

1. INTRODUCTION

1.1 General

The importance of energy conservation has been a driving force behind the ongoing research that will reduce the drag on transport vehicles. Passive control of the flow field around the body may result in aerodynamic drag reduction and a conforming performance enhancement.

Surface roughness has been widely investigated as a means of modifying the turbulent boundary layer. It is assumed that the Transverse Square Grooves create a low-pressure area immediately downstream, which sucks fluid back from the main flow, creating a circulating vortex prolonging the turbulent development in the boundary layer [5], thus controlling the boundary layer separation over the body. In 2-dimensional flow the boundary layer separates at the point in the flow where the shear stress on the wall is almost zero and the flow changes into turbulent [3]. Passive and active maneuvering of the flow field may produce drag reduction which causes increase in the performance.

Not in distant past, friction drag reduction methods have gained popularity in relation to less fuel consumption in aircrafts and submarines. Reduction using riblets have drawn more attention due to their greater potential of reducing drag.

1.2 Flat Plate

Square grooves are comparatively easier to develop than a riblet surface. These 2-dimensional square grooves are placed in transverse to the incoming flow. They are more suitable for any further optimization, and when added together, they can further lessen the skin-friction drag. Refrigeration systems, plate heat exchangers and other engineering equipment's use large grove designs [4]. Whereas bearings, automobiles, breaking system and high-pressure equipment's use microscopic grooves.

Contradictory results have been recorded regarding the effectiveness of square grooves [3]. It has been suggested that transverse square grooves, optimally sized and located, could result in skin-friction drag reduction. [5].

1.3 Ahmed Body

In this study a base line drag value is obtained for a Dumper Truck using a Square Back Ahmed Body in Ansys Fluent and the drag reduction through different modifications in the groove design along the Dumper Body are compared.

The market does not appreciate frequent launching of new models. New truck model demands more time to design and are not affordable for Pakistani buyers. According to a study conducted in Pakistan, aerodynamic pressure drag leads up to 15-20 % of extra fuel consumption [6]. There is a probability that the aerodynamic drag of Dumper Trucks in developing countries like Pakistan can lead to great profit by reducing the fuel consumption.

The corner of vehicles with square back causes the air fleeting by its body to separate, leading to a massive fall in the pressure that produces a long wake behind the vehicle [7], [8]. The target of this study is to develop control solution to reduce the aerodynamic drag of the vehicle without forcing a change in the original design of the body. The success depends upon controlling the point where the separation along the body occurs. Recirculation area at the rear end of the body can be cut down by installing separation accessories at the back or the front of the body.

Intriguing results were achieved with grooves positioned along the boundary, transverse to the incoming flow [9], [10]. This creates a force along the boundary layer which helps shift the separation point resulting in a decrease in pressure drag and decreasing the aerodynamic drag is another effective solution [7], [11]. Besides, the use of artificial rough surface achieves up to 50% reduction in drag. Turbulent laminar transition can also be rushed by using self-adapting surfaces made of special coating [12], [13]. The flow is naturally turbulent in automobile aerodynamics, thus the impact is very low.

2. METHODOLOGY

In the first phase two different configurations of flat plate are simulated and validated through literature. These 2 different configurations consist of*; **1)** Flat plat with smooth wall, **2)** Flat Plate with single square groove.*

In the second phase these configurations of grooves are simulated on an Ahmed Body which is compared to a bluff body such as a heavy transport vehicle [14], [11]. Recirculation zones are created due to the separations occurring along the body, resulting in huge drag coefficient. The objective of this paper is to control or reduce the separation area in the wake. A 2-Dimensional study is performed in which we concentrate on the total pressure gradient that governs the aerodynamic drag of Square Back Ahmed Body, which is a simplified form of Dumper Truck.

The use of Transverse Square grooves is a new possibility that can modify the boundary layer behavior. Here the flow control is achieved by means of Transverse Square groove which are inserted on the surface of the body. These square grooves modify the boundary layer effect as it changes the stress forces [15], [16]. The goal is to show how well positioned transverse grooves and their geometry can modify the wake.

In the following we give various results of different configuration of the flat plate and the flow on square back Ahmed Body. We carefully analyze these results and assess the effect of Square Grooves in the flow around the body.

3. GEOMETRICAL DIMENSION

3.1 Flat Plate

Smooth wall

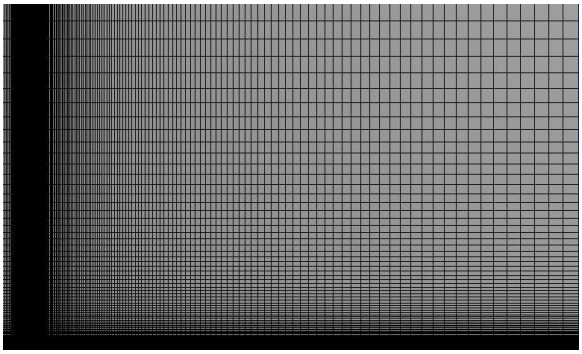

Figure 1 Flat Plate Smooth Wall Mesh

Domain Length	1.75m
Domain Height	1m
Plat Length	1.7m
Inlet Velocity	5.4 mps
Turbulent Intensity	5%
Turbulent Viscosity Ratio	10

Flat Plat with Single Square Groove

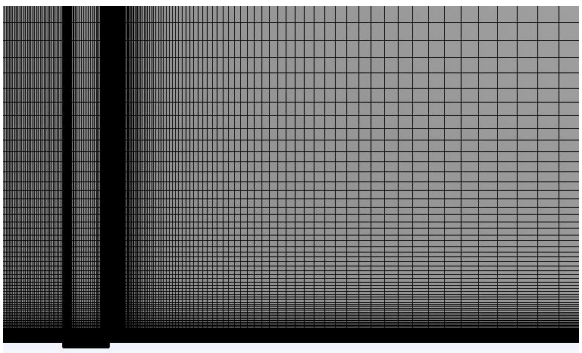

Figure 2 Flat Plate Single Groove Mesh

Domain Length	1.75m
Domain Height	1m
Plat Length	1.7m
Groove Depth	0.014m
Groove Length	0.14m
Inlet Velocity	5.4 mps
Turbulent Intensity	5%
Turbulent Viscosity Ratio	10

3.2 Ahmed Body

Smooth Wall

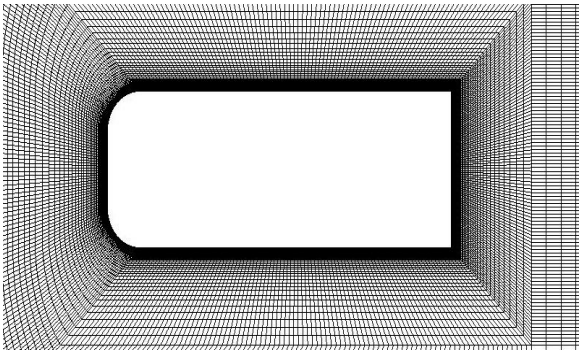

Figure 3 Smooth Wall Ahmed Body Mesh

Domain Length	6.79m
Domain Height	2.33m
Ahmed Body Length	1.044m
Ahmed Body Width	0.39m
Front Filet Raduis	0.10m
Inlet Velocity	5.4 mps
Turbulent Intensity	5%
Turbulent Viscosity Ratio	10

Square Grooves at Rear End

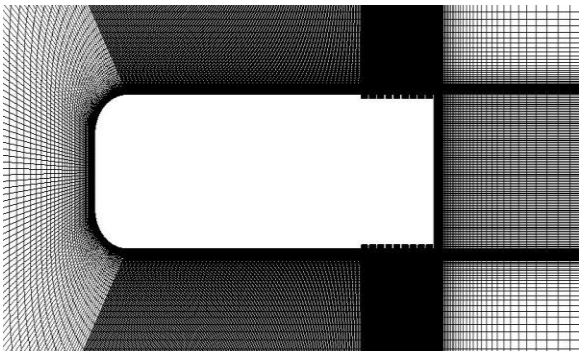

Figure 4 Grooved Wall Ahmed Body Mesh

Domain Length	6.79m
Domain Height	2.33m
Ahmed Body Length	1.044m
Ahmed Body Width	0.39m
Front Filet Raduis	0.10m
Groove Depth	0.01m
Groove length	0.02m
Distance between Grooves	0.005m
Inlet Velocity	5.4 mps
Turbulent Intensity	5%
Turbulent Viscosity Ratio	10

4. Grid Independence

Grid independence test is performed to ensure that mesh size does not affect the simulation outcomes. Pressure Coefficient is monitored inside the domain to investigate the convergence history.

Three different mesh are considered by changing the number of nodes along the geometry, resulting in the increase of elements. Number of elements and its effect on Pressure coefficient are discussed below.

Number of Elements	Pressure Coefficient C_f
20,098	0.357
59,998	0.545
90,298	0.547

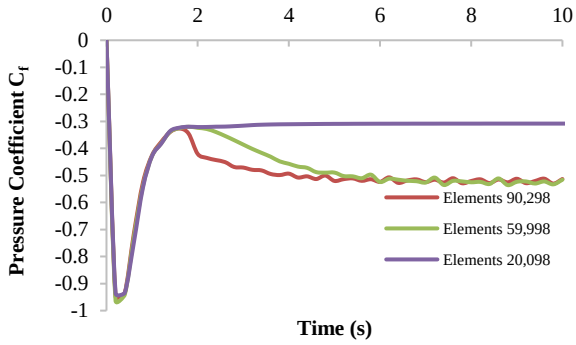

Graph 1 Pressure Coefficient vs Time at Different Number of Elements

Graph 1 shows that the resulting pressure coefficient for elements 59,998 and above is constant but as we decrease the number of elements to 20,098, divergence starts to occur.

5. RESULTS

5.1 Flat Plate

It can be seen from the graph and validated through literature that there is an overshoot just downstream of the groove followed by an undershoot

and an oscillatory relaxation back to the smooth- wall value [3].

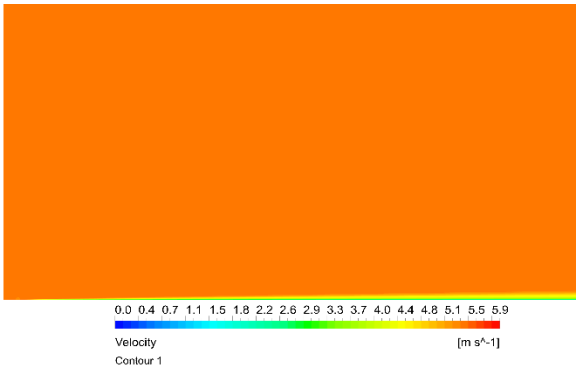

Figure 5 Flat Plate Smooth Wall Velocity Contours

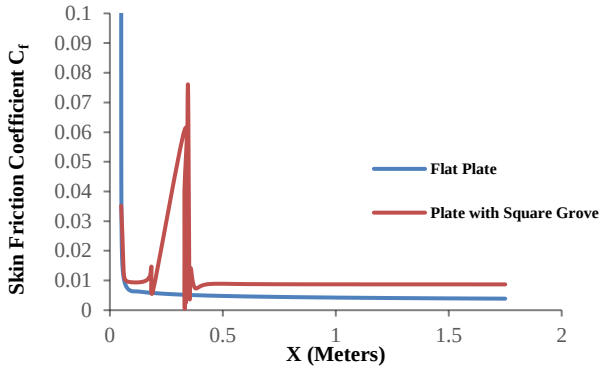

Graph 2 Smooth vs Grooved Wall Skin friction

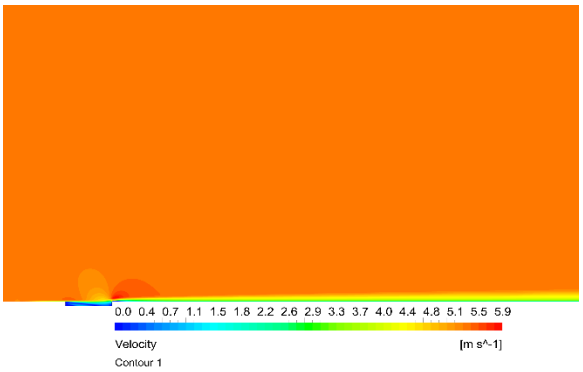

Figure 6 Grooved Flat Plate Velocity Contours

Fig 5 and 6 are the velocity contours of the simulations performed on the Smooth wall Flat Plate and Grooved Wall Flat Plate respectively.

Graph 2 shows the graph between Skin Friction Coefficient and the Length along the flat plate. It is quite visible that there is an abrupt increase in the skin friction coefficient as the incoming flow passes through the Square Groove. This increased skin friction helps in making the flow transition from laminar to turbulent and reduces the length of the separation which helps the flow to stay attached with the body for a longer time, hence reducing the wake.

5.2 Ahmed Body

Simulation are performed on an Ahmed Body with a smooth wall and Square Grooves at the rear end of the Ahmed Body.

Firstly, the simulations run on a Smooth Wall Ahmed Body and the Coefficient of Drag was noted. After that Transverse Square Grooves of equal size were created and equally spaced apart at the rear end of the Ahmed Body.

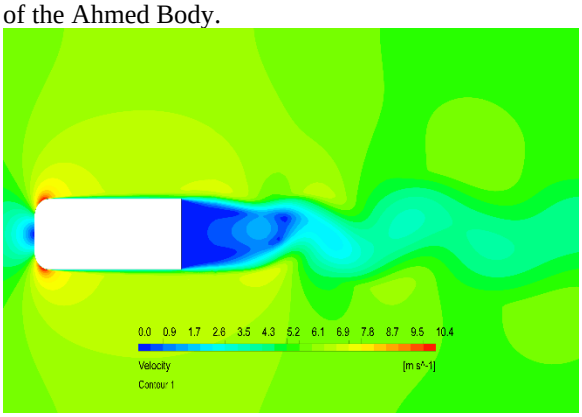

Figure 7 Smooth Wall Ahmed Body Velocity Contour

Fig 7 shows the Velocity contours of the Ahmed Body with Smooth Wall surface. The Blue region behind the body represents the wake created due to the pressure difference between the front and rear end of the body.

After creating Transverse Square Grooves, simulations with the same boundary conditions were run to compare the difference in the wake before and after the grooves were created.

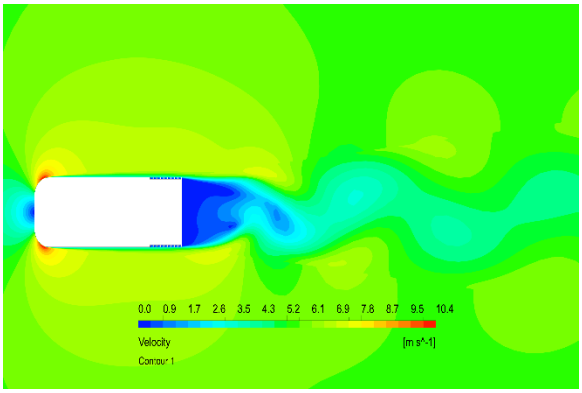

Figure 8 Grooves at the rear end of Ahmed Body Velocity Contour

Fig 8 represents the wake length is decreased due to the creation of grooves at the rear end of the body. Due to limited computational power a minor difference in the wake is captured.

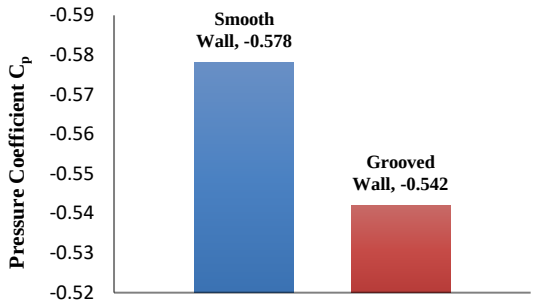

Graph 3 Smooth vs Grooved Wall Coefficient of Pressure

Graph 3 informs us about the mean pressure coefficient taken at a point behind the square back Ahmed Body at (1.2, 0.2, 0) in both domains. The mean pressure coefficient of Smooth wall Ahmed Body jumps from -0.578 to -0.542 of Grooved wall Ahmed Body with an increment of 6.22 %, resulting in the drop of pressure drag.

This difference is made more visually clear by including the streamline in the velocity contours as shown in the Fig 9 and 10.

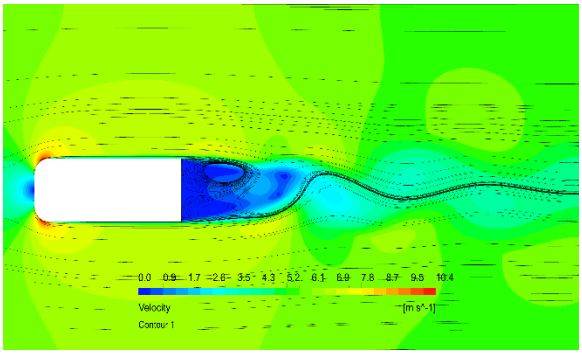

Figure 9 Smooth wall Ahmed Body Streamline Velocity Contour

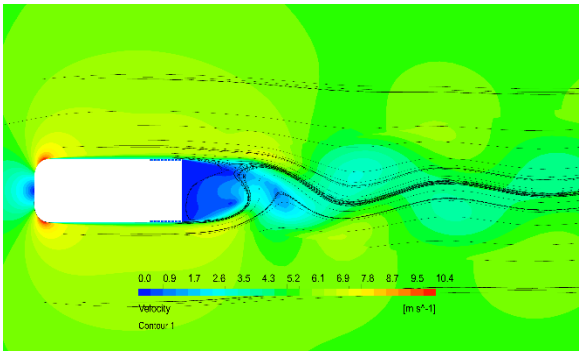

Figure 10 Grooved wall Ahmed Body Streamline Velocity Contour

In the Fig 9 and 10 the streamlines in velocity contours are used to demonstrate the recirculation of flow behind the body, before and after the creation of Transverse Square grooves.

The density of these streamline at the back indicates that the recirculation of the flow at the back of Smooth walled Ahmed body is larger than the Grooved Ahmed Body, hence the wake created on smooth Ahmed body is greater.

REFERENCES

[1] M. A. Choudhary, N. Khan, M. Arshad, and A. Abbas, "Analyzing Pakistan ' s Freight Transportation Infrastructure Using Porter ' s Framework and Forecasting Future Freight Demand Using Time Series Models."

[2] G. Siva and V. Loganathan, "Design and Aerodynamic Analysis of a Car to Improve Performance," vol. 24, pp. 133–140, 2016.

[3] R. Wahidi and W. Chakroun, "The behavior of the skin-friction coefficient of a turbulent boundary layer flow over a flat plate with differently configured transverse square grooves," vol. 30, pp. 141–152, 2005.

[4] D. M. Bushnell and J. N. Hefner, Viscous Drag Reduction in Boundary Layers Edited by. .

[5] "The effect of a square groove on a boundary layer.pdf." .

[6] B. Data and A. Series, "SHORT ROUNDUP ON TRANSPORT INFRASTRUCTURE IN," 2016.

[7] R. S. Khan and S. Umale, "CFD Aerodynamic Analysis of Ahmed Body," vol. 18, no. 7, pp. 301–308, 2014.

[8] G. Vehicle, C. Bruneau, and E. Creus, "Analysis of the Active and Passive Drag Reduction Strategies Behind a Square Back Analysis of the Active and Passive Drag Reduction Strategies Behind a Square Back Ground Vehicle," no. August 2016, 2018.

[9] C. Bruneau, E. Creusé, D. Depeyras, P. Gilliéron, and I. Mortazavi, "Computers & Fluids Coupling active and passive techniques to control the flow past the square back Ahmed body," Comput. Fluids, vol. 39, no. 10, pp. 1875–1892, 2010.

[10] "Effect of compressibility on the global stability of axisymmetric wake flows," vol. 660, pp. 499–526, 2010.

[11] "Passive Control Around the Two-Dimensional Square Back Ahmed Body Using Porous," vol. 130, no. June 2008, pp. 1–12, 2016.

[12] P. W. Bearman and J. K. Harveyt, "Control of Circular Cylinder Flow by the Use of Dimples," vol. 31, no. 10, pp. 2–5, 1993.

[13] B. Pw, "Investigation of the flow behind a two-dimensional model with a blunt trailing edge and fitted with splitter plates," vol. 21, pp. 241–255, 1965.

[14] G. Luiz, O. Halila, and S. A. Embraer, "A Numerical Study On Transitional Flows by Means of a Correlation-Based Transition Model," no. January, pp. 1–34, 2015.

[15] M. J. Walsh, "Riblets as a Viscous Drag Reduction Technique," vol. 21, no. 4, pp. 1–5, 1983.

[16] W. Engineering and I. Aerodynamics, "Reynolds-number effects in flow around more-or-less bluff bodies," vol. 89, pp. 1267–1289, 2001.